Eur. Phys. J. C (2014) 74:2871
DOI 10.1140/epjc/s10052-014-2871-x

THE EUROPEAN PHYSICAL JOURNAL C

Regular Article - Theoretical Physics

Large N approach to Kaon decays and mixing 28 years later: $\Delta I = 1/2$ rule, $\hat{B}_K$, and ΔM_K

Andrzej J. Buras[1,2,a], **Jean-Marc Gérard**[3], **William A. Bardeen**[4]

[1] TUM Institute for Advanced Study, Lichtenbergstr. 2a, 85747 Garching, Germany
[2] Physik Department, Technische Universität München, James-Franck-Straße, 85747 Garching, Germany
[3] Centre for Cosmology, Particle Physics and Phenomenology (CP3), Université catholique de Louvain, Chemin du Cyclotron 2, 1348 Louvain-la-Neuve, Belgium
[4] Fermilab, P.O. Box 500, Batavia, IL 60510, USA

Received: 10 February 2014 / Accepted: 24 April 2014 / Published online: 20 May 2014

Abstract We review and update our results for $K \to \pi\pi$ decays and K^0–$\bar{K}^0$ mixing obtained by us in the 1980s within an *analytic* approximate approach based on the dual representation of QCD as a theory of weakly interacting mesons for large N, where N is the number of colors. In our analytic approach the Standard Model dynamics behind the enhancement of $\mathrm{Re}A_0$ and suppression of $\mathrm{Re}A_2$, the so-called $\Delta I = 1/2$ rule for $K \to \pi\pi$ decays, has a simple structure: the usual octet enhancement through the long but slow quark–gluon renormalization group evolution down to the scales $\mathcal{O}(1\ \mathrm{GeV})$ is continued as a short but fast meson evolution down to zero momentum scales at which the factorization of hadronic matrix elements is at work. The inclusion of lowest-lying vector meson contributions in addition to the pseudoscalar ones and of Wilson coefficients in a momentum scheme improves significantly the matching between quark–gluon and meson evolutions. In particular, the anomalous dimension matrix governing the meson evolution exhibits the structure of the known anomalous dimension matrix in the quark–gluon evolution. While this physical picture did not yet emerge from lattice simulations, the recent results on $\mathrm{Re}A_2$ and $\mathrm{Re}A_0$ from the RBC-UKQCD collaboration give support for its correctness. In particular, the signs of the two main contractions found numerically by these authors follow uniquely from our analytic approach. Though the current–current operators dominate the $\Delta I = 1/2$ rule, working with matching scales $\mathcal{O}(1\ \mathrm{GeV})$ we find that the presence of QCD-penguin operator Q_6 is required to obtain satisfactory result for $\mathrm{Re}A_0$. At NLO in $1/N$ we obtain $R = \mathrm{Re}A_0/\mathrm{Re}A_2 = 16.0 \pm 1.5$ which amounts to an order of magnitude enhancement over the strict large N limit value $\sqrt{2}$. We also update our results for the parameter $\hat{B}_K$, finding $\hat{B}_K = 0.73 \pm 0.02$. The smallness of $1/N$ corrections to the large N value $\hat{B}_K = 3/4$ results within our approach from an approximate cancelation between pseudoscalar and vector meson one-loop contributions. We also summarize the status of ΔM_K in this approach.

1 Introduction

Flavor violating transitions involving K mesons have played a very important role since their discovery in 1950s, both in the construction of the Standard Model (SM) and more recently in the tests of its possible extensions. Unfortunately, due to non-perturbative uncertainties only rare K decays like $K^+ \to \pi^+\nu\bar{\nu}$ and $K_L \to \pi^0\nu\bar{\nu}$ can be considered as theoretically clean, that is, not suffering from hadronic uncertainties. But here we still have to wait for sufficiently precise experimental results in order to see whether the SM agrees with experimental data or not.

On the other hand a number of observables in $K \to \pi\pi$ decays and K^0–$\bar{K}^0$ mixing have been measured very precisely already for quite some times. In quoting their values we follow the conventions and normalizations of [1]. In particular, we have the following.

- The real parts of the amplitudes A_I for a Kaon to decay into two pions with isospin I are measured to be [2]

$$\begin{aligned} \mathrm{Re}A_0 &= 27.04(1) \times 10^{-8}\ \ \mathrm{GeV}, \\ \mathrm{Re}A_2 &= 1.210(2) \times 10^{-8}\ \ \mathrm{GeV}, \end{aligned} \tag{1}$$

and they express the so-called $\Delta I = 1/2$ rule [3,4]

$$R = \frac{\mathrm{Re}A_0}{\mathrm{Re}A_2} = 22.35. \tag{2}$$

[a] e-mail: aburas@ph.tum.de

- The experimental value for the $K_L - K_S$ mass difference is

$$(\Delta M_K)_{\rm exp} = 3.484(6)10^{-15}\,{\rm GeV}. \tag{3}$$

- The parameter ε_K, a measure of indirect CP-violation in $K_L \to \pi\pi$ decays, is found to be

$$\varepsilon_K = 2.228(11) \times 10^{-3} e^{i\phi_\varepsilon}, \tag{4}$$

where $\phi_\varepsilon = 43.51(5)^\circ$.

- The ratio of the direct CP-violation and indirect CP-violation in $K_L \to \pi\pi$ decays is measured to be [2,5–7]

$${\rm Re}(\varepsilon'/\varepsilon) = 1.65(26) \times 10^{-3}. \tag{5}$$

In the second half of the 1980s we have developed an approach to K^0–$\bar{K}^0$ mixing and non-leptonic K-meson decays [8–12] based on the dual representation of QCD as a theory of weakly interacting mesons for large N, where N is the number of colors [13–16]. Reviews of our work can be found in [17–23]. This approach provided, in particular, first results within QCD for the amplitudes ${\rm Re}A_0$ and ${\rm Re}A_2$ in the ballpark of experimental values. In this manner, for the first time, the SM dynamics behind the $\Delta I = 1/2$ rule has been identified. In particular, it has been emphasized that at scales $\mathcal{O}(1\ {\rm GeV})$ long-distance dynamics in hadronic matrix elements of current–current operators and not QCD-penguin operators, as proposed in [24], are dominantly responsible for this rule. Moreover, it has been demonstrated analytically why ${\rm Re}A_0$ is enhanced and why ${\rm Re}A_2$ is suppressed relative to the vacuum insertion approximation (VIA) estimates. In this context, we have emphasized that the so-called Fierz terms in the latter approach totally misrepresent $1/N$ corrections to the strict large N limit for these amplitudes.

Our approach allowed us also to calculate, for the first time within QCD, the non-perturbative parameters $\hat{B}_K$, $B_6^{(1/2)}$, and $B_8^{(3/2)}$ governing the corresponding matrix elements of $\Delta S = 2$ SM current–current operator and $K \to \pi\pi$ matrix elements of the dominant QCD-penguin (Q_6) and the dominant electroweak penguin (Q_8) operators. Both parameters are crucial for the evaluation of ε'/ε within the SM and its various extensions. Also the $K \to \pi\pi\pi$ decays have been analyzed in [25] and the $K_L - K_S$ mass difference ΔM_K including long-distance contributions has been calculated [21,26] within this approach. During the last two decades some of these calculations have been improved and extended. Other applications of large N ideas to $K \to \pi\pi$ and $\hat{B}_K$, but in a different spirit from our original approach, are reviewed in [1]. We refer in particular to [27–35]. Recent review of $SU(N)$ gauge theories at large N can be found in [36].

In view of the recent advances by lattice QCD on several of these parameters [37–43], we think it is useful to improve and update our old results and confront them with the latter. We hope that our analytic approach will shed light on the dynamics behind the numerical lattice computations which appear to indicate a pattern of long-distance QCD effects in $K \to \pi\pi$ amplitudes and K^0–$\bar{K}^0$ mixing that is very similar to the one identified by us long time ago.

In fact, as we will discuss in more detail in the context of our presentation, the recent lattice results show the following.

- The parameter $\hat{B}_K$ is close to its large N limit, $\hat{B}_K \approx 0.75$, as found by us in [12].
- The amplitude ${\rm Re}A_2$ is suppressed through two contributions (contractions) having opposite sign and the data are reproduced within 15 %. This pattern has been identified already in [11] and we will demonstrate analytically that these signs follow directly from our approach.
- Both in the case of ${\rm Re}A_2$ and $\hat{B}_K$ our findings of 1980s that VIA misrepresents QCD have been recently confirmed not only for ${\rm Re}A_2$ in [37] but in the case of $\hat{B}_K$ also in [44]. This is an important confirmation as in 1988 lattice results provided $\hat{B}_K \approx 1$ [45] in contradiction with the negative correction to the large N limit for $\hat{B}_K$ found by us [12]. See also [46] were the upper bound $\hat{B}_K \le 0.75$ has been derived.
- The amplitude for ${\rm Re}A_0$ is enhanced through the contractions encountered in ${\rm Re}A_2$ entering this time the amplitude with the same sign. In this manner another of our findings of 1980s has been confirmed. Unfortunately, as ${\rm Re}A_0$ from lattice QCD is presently only available for non-physical kinematics, the size of this enhancement is not precisely known. Consequently a comparison between our and lattice results in this case is difficult at present.

While according to these findings it appears that an understanding of the $\Delta I = 1/2$ rule is emerging from lattice QCD [37,47], we would like to emphasize that the suppression of ${\rm Re}A_2$, while important, is in fact a subleading fraction of this rule. It is the enhancement of ${\rm Re}A_0$ that is responsible dominantly for the $\Delta I = 1/2$ rule. Indeed, without short-distance and long-distance QCD effects $R \to \sqrt{2}$ and

$$\begin{aligned} {\rm Re}A_0 &\to 3.59 \times 10^{-8}\ {\rm GeV}, \\ {\rm Re}A_2 &\to 2.54 \times 10^{-8}\ {\rm GeV}, \qquad \text{(in large } N \text{ limit)} \end{aligned} \tag{6}$$

in plain disagreement with the data in (1) and (2). The explanation of the missing enhancement factor of 15.8 in R through QCD dynamics must simultaneously give the correct values for ${\rm Re}A_0$ and ${\rm Re}A_2$. This means that this dynamics should suppress ${\rm Re}A_2$ by a factor of 2.1, not more, and it

should enhance $\mathrm{Re}A_0$ by a factor of 7.5. In our view, the understanding of this large enhancement of $\mathrm{Re}A_0$ did not yet emerge from lattice QCD but has been identified at a reduced level (5 ± 1) in our approach in 1986. We will demonstrate this in explicit terms below, improving significantly on our original estimates.

Our paper is organized as follows. In Sect. 2 we make a brief historical review of applications of our large N framework to weak decays of mesons. We think this is necessary as many of the useful and important results obtained in this framework in the last 30 years appear to be unknown to younger generations, in particular in the lattice community. Indeed several of the results obtained in our papers have been confirmed in the last years by lattice calculations numerically with higher control over uncertainties than it was possible in the 1980s, partly due to the fact that the value of α_s was not precisely known at that time. In Sect. 3 we recall the basic ingredients of the large N approach to weak decays formulated in [8–12] that is based on the dual description of QCD at large distance scales as a truncated meson theory in which only pseudoscalar meson contributions were taken into account. In Sect. 4 we generalize this approach to include the effects of vector meson contributions [21,48]. This section is important as it gives further support to our approach. Indeed the inclusion of vector meson contributions improves significantly the matching between quark–gluon and meson pictures at scales $\mathcal{O}(1\ \mathrm{GeV})$. This matching is then discussed in more detail in Sect. 5. Calculating the Wilson coefficients at NLO in a momentum scheme clarifies the relation between the relevant scales M and μ in the effective and full theories.

It is strategically useful to illustrate our approach by discussing first the $\hat{B}_K$ parameter. This we do in Sect. 6 including first pseudoscalar meson contributions and subsequently vector meson contributions. Armed with this technology we discuss in Sect. 7 the $\mathrm{Re}A_0$ and $\mathrm{Re}A_2$ amplitudes, concentrating on current–current operators and summarizing briefly the status of the parameters $B_6^{(1/2)}$ and $B_8^{(3/2)}$ associated with penguin operators. With this information at hand we describe in Sect. 8 the understanding of the $\Delta I = 1/2$ rule within our approach. We also improve and update the numerical analysis of $\mathrm{Re}A_0$ and $\mathrm{Re}A_2$, including both current–current and penguin contributions. Again, the inclusion of vector meson contributions turns out to be important for our final results. In Sect. 9 we compare our results from dual QCD to those available from lattice QCD. In particular the signs of various contributions found numerically by the RBC-UKQCD lattice collaboration provide the confirmation of our analytic results of 1980s. Moreover, our approach allows an understanding of the origin of these signs, which is difficult in the lattice approach. In Sect. 10 we focus on the $K_L - K_S$ mass difference and briefly mention other applications. We conclude in Sect. 11.

2 Historical review of large N applications to weak decays

The first attempts to apply $1/N$ expansion to weak decays can be found in [49–51]. However, the first big step forward in the phenomenological applications of this expansion has been made in [52] in the context of non-leptonic charm decays, where it was realized that removing the $1/N$ Fierz terms from the usual vacuum insertion approximation softened the disagreement of the theory with both exclusive and inclusive data[1] This simple philosophy of using the $1/N$ expansion has been subsequently applied to $K \to \pi\pi$ decays, ΔM_K, and ε_K in [8]. The first leading order results for the matrix elements of operators relevant for these observables can be found in this paper. Probably the most important results in this paper are $\hat{B}_K = 3/4$[2] and the realization that the removal of $1/N$ Fierz terms from vacuum insertion calculations of current–current matrix elements suppresses $\mathrm{Re}A_2$, moving the theory in the direction of the data. In this paper also the first large N result for the matrix elements of the dominant QCD-penguin operator Q_6 can be found. These leading order results have been subsequently confirmed in [9,10] by using an effective Lagrangian describing the weak and strong interactions of mesons in the large N limit. In particular, it has been emphasized in [10] that a consistent evaluation of the $K \to \pi\pi$ amplitudes should include two contributions:

- The evolution from M_W down to $\mu \approx \mathcal{O}(1\ \mathrm{GeV})$, termed *quark–gluon evolution*, by means of the usual renormalization group equations. The result of this evolution are the values of the Wilson coefficients of local operators at $\mu \approx \mathcal{O}(1\ \mathrm{GeV})$.
- The continuation of this evolution down to $\mu = \mathcal{O}(m_\pi)$ within a meson theory dual to QCD, termed *meson evolution*. The result of this evolution are factorizable hadronic matrix elements.

In [10] details of quark–gluon evolution in the $1/N$ approach have been presented. In particular, it has been shown how the usual very complicated renormalization group analysis simplifies for large N, still reproducing well the exact results. In this paper an additional (with respect to previous estimates) enhancement of the QCD-penguin contribution to $\mathrm{Re}A_0$ has been identified. It comes from an incomplete GIM cancelation above the charm quark mass. In lattice calculations that work at scales $\mu = (2\text{–}3)$ GeV, which are well above that mass, GIM is still rather powerful and the bulk of this contribution should be present in the

[1] This procedure has been motivated by the analysis in [53]. However, these authors did not attach it with a consistent application of the $1/N$ expansion.

[2] See also [54].

matrix elements of current–current operators. Strategies for including charm quark contributions in lattice calculations in the context of the $\Delta I = 1/2$ rule and the $K_L - K_S$ mass difference have been presented in [55,56] and [57], respectively.

Our studies of the 1980s culminated in the formulation of the meson evolution in [11,12] and evaluation in this framework of $1/N$ corrections to $K \to \pi\pi$ amplitudes and the parameter $\hat{B}_K$. These papers represent the first attempt at a consistent calculation of the weak matrix elements in the continuum field theory. Pedagogical summary of this work has been presented by the authors in various reviews and lectures [17–23].

3 Large N approach to weak decays of mesons

3.1 General structure

Let us begin our presentation with the general formula for the $K \to \pi\pi$ decay amplitudes in the Standard Model [58]

$$A(K \to \pi\pi) = \frac{G_F}{\sqrt{2}} V_{ud} V_{us}^* \sum_{i=1}^{10} (z_i(\mu) + \tau y_i(\mu)) \langle \pi\pi | Q_i(\mu) | K \rangle \tag{7}$$

where

$$\tau = -\frac{V_{td} V_{ts}^*}{V_{ud} V_{us}^*}. \tag{8}$$

The coefficients $z_i(\mu)$ and $y_i(\mu)$ are the Wilson coefficients of local four-quark operators. The complete set of these operators listed in [58] consists of current–current operators $Q_{1,2}$, QCD-penguin operators Q_3–Q_6 and electroweak penguin operators Q_7–Q_{10}. In our presentation only five of them will be relevant, namely Q_1, Q_2, Q_4, Q_6, and Q_8. For our discussion it is useful to write them in the Fierz transformed form relative to the ones in [58]. They are constructed from the light fields only $q = (u, d, s)$ and are given as products of color-singlet densities, as follows:

$$Q_1 = 4(\bar{s}_L \gamma_\mu d_L)(\bar{u}_L \gamma_\mu u_L),$$
$$Q_2 = 4(\bar{s}_L \gamma_\mu u_L)(\bar{u}_L \gamma_\mu d_L), \tag{9}$$
$$Q_6 = -8(\bar{s}_L q_R)(\bar{q}_R d_L),$$
$$Q_8 = -12 e_q (\bar{s}_L q_R)(\bar{q}_R d_L), \tag{10}$$
$$Q_4 = 4(\bar{s}_L \gamma_\mu q_L)(\bar{q}_L \gamma_\mu d_L) \tag{11}$$

where $q_{R(L)} = (1/2)(1 \pm \gamma_5) q$ and sums over color indices and q in Q_4, Q_6 in Q_8 are understood. Evidently, $Q_{1,2}$ are current–current operators, whereas Q_6 and Q_8 are the dominant density–density QCD-penguin and electroweak penguin operators, respectively. The subleading QCD-penguin operator Q_4 will only play a role in our discussion of the matching of meson and quark–gluon evolutions. Finally, the operator relevant for K^0–$\bar{K}^0$ mixing will be given in Sect. 6, but the approach below applies in this case as well.

Since the operators Q_i in (9)–(11) are constructed from the light quark fields only, the full information about the heavy quark fields (c, b, t) is contained in the Wilson coefficients z_i and y_i. Correspondingly, the normalization scale μ in (7) is not completely arbitrary in our approach but must be chosen below the charm quark mass. The values of $z_i(\mu)$ and $y_i(\mu)$ have been calculated in 1993 at the NLO level in the renormalization group improved perturbation theory including both QCD and QED corrections [58,59]. Also some elements of NNLO corrections can be found in the literature [60,61].

In the large N approach of [8–12] the structure of different contributions to physical amplitudes is as follows. The physics contributions from scales above μ are fully contained in the coefficients $z_i(\mu)$ and $y_i(\mu)$, whereas the remaining contributions from the low-energy physics below μ (i.e. from μ to the factorization scale expected around m_π) are contained in the matrix elements $\langle \pi\pi | Q_i(\mu) | K \rangle$. It follows that for $\mu = \mathcal{O}(1\ \text{GeV})$, the coefficients $z_i(\mu)$ and $y_i(\mu)$ can be calculated within a perturbative *quark–gluon picture* by means of renormalization group methods [62].

As far as the meson matrix elements are concerned, the ultimate goal is to compute them in a non-perturbative quark–gluon picture where mesons occur as bound states. This route is followed by lattice computations and in fact since our work appeared in 1986 impressive progress has been made in this manner [41–43]. Yet this numerical route is very demanding as even after more than a quarter of a century of hard work by lattice community the present results for $K \to \pi\pi$ amplitudes are still not fully satisfactory and the matrix element $\langle \pi\pi | Q_6(\mu) | K \rangle$ from lattice QCD is presently unknown. Moreover, it is much harder to understand the underlying physics than by means of an analytic approach.

Our proposal, summarized most explicitly, in [11] was to apply instead the ideas of 't Hooft [13,14] and subsequently Witten [15,16] to non-leptonic K decays and K^0–$\bar{K}^0$ mixing. They conjectured that QCD (the theory of quarks and gluons) is for large N equivalent to a theory of weakly interacting mesons with a quartic meson coupling being $\mathcal{O}(1/N)$. This allows us to formulate a dual representation of the strong dynamics in terms of hadronic degrees of freedom. In the large N limit, this representation becomes exact and a full description of the physics can be achieved using an infinite set of interacting meson fields.

The fact that QCD can be formulated both as theory of quarks and gluons on the one hand and as the theory of mesons on the other hand can now be used for Kaon mixing and non-leptonic decays $K \to \pi\pi$ as follows. The main point is that the matrix elements of four-fermion operators governing these transitions can be written at leading order in

large N as products of matrix elements of color-singlet currents in the case of current–current operators and as products of matrix elements of quark densities in the case of penguin operators. At the next-to-leading order one has two classes of contributions:

- $1/N$ corrections to the matrix elements of factorized operators.
- Low-energy, non-factorized matrix elements of two currents or two quark densities.

The latter contributions can be written as an integral over the momentum flowing through the currents (densities) in the connected planar amplitude. One can then use knowledge of both the high- and the low-energy behavior of the integrand. At high momentum, these are just the short-distance contributions to the coefficient functions of the operator product expansion which can be computed perturbatively in the quark–gluon picture. While in principle this could also be done in the *meson picture*, such an analysis would be very complex requiring many meson states and complicated interactions. However, the long-distance analysis is correspondingly simple as only lowest-lying meson states may be required and the interactions are largely dictated by the chiral symmetry structure of the effective Lagrangian.[3] Our proposal in [11] was to use the meson theory to interpolate to the point where one can match the behavior of the integrand of the short-distance theory. If the amplitude is smooth enough then it may be sufficient to match the meson amplitude to the quark amplitude at an appropriate scale. In this manner one can achieve a consistent unified description of the physics by using the quark–gluon picture at short distances matched to the meson picture at long distances. The accuracy of the method depends on the interpolation of the integrand between short and long distance.

A full AdS/QCD description [64,65] should be able to interpolate the meson amplitudes to arbitrarily short distance and first attempts in this direction have been made in [66,67]. In our approach the matching scale must presently be chosen around 1 GeV implying approximate treatments in both pictures. In particular, the scheme dependence of the long-distance part comes when one subtracts the short-distance part of the integral using a particular scheme. This scheme dependence can be treated exactly if needed. In this context, calculating Wilson coefficients and the hadronic matrix elements in a momentum scheme we have made in the present paper a significant progress relative to our previous papers. We will discuss this important issue in Sects. 5 and 8.

[3] Moreover, the spontaneous breakdown of chiral symmetry $SU(3)_L \times SU(3)_R \to SU(3)_V$ can be proven to be true in QCD in its large N limit [63].

In spite of not being exact, this approach has several virtues. Indeed, the simplicity of this formulation lies in the fact that in the strict large N limit QCD becomes a free theory of mesons and consequently the leading order contributions to any quantity are obtained by calculating tree diagrams with the propagated objects being mesons, not quarks or gluons. In this strict limit, also the factorization of hadronic matrix elements of four-quark operators into the product of matrix elements of quark currents or quark densities follows. Beyond this limit, one obtains $1/N$ expansion represented by a loop expansion in the meson theory. Even if naively these corrections could be expected to be small, one should notice that one-loop contributions in the meson theory represent in fact the leading term in the $1/N$ expansion for observables like the $\pi^+ - \pi^-$ electromagnetic mass difference or the K^0 decay into two neutral pions. In particular, they have to be sizable if one wants to explain why the subleading $K^0 \to \pi^0\pi^0$ decay amplitude turns out to be almost equal to the $K^0 \to \pi^+\pi^-$ leading one, namely the so-called $\Delta I = 1/2$ rule.

We close this section by discussing briefly the issue of matching between the quark–gluon and meson theories. We will discuss this crucial issue more explicitly in Sects. 5 and 8. In the quark–gluon picture, the scale μ enters naturally as the normalization scale in the renormalization group improved perturbative QCD calculations

$$\mu^2 \frac{\mathrm{d}}{\mathrm{d}\mu^2} Q_i(\mu^2) = -\frac{1}{2}\gamma_{ij} Q_j(\mu^2) \tag{12}$$

with γ, the anomalous dimension matrix for the Q_i operators. In our formulation, it serves as an infrared cutoff below which one should switch to the meson picture unless one wants to perform lattice computations. Now the truncated meson theory, involving a finite set of light pseudoscalar and vector mesons only, appears non-renormalizable. In particular, if only lowest-lying pseudoscalar mesons are included without ultraviolet QCD completion, it exhibits a quadratic dependence on the cutoff, which we will denote by M. This *physical* cutoff must be introduced in order to restrict the truncated meson theory to the long-distance domain or, in other words, to cut off the high mass and high momentum contributions in the meson loops. Therefore, the physical cutoff introduced here should be distinguished from the usual cutoff regularization procedure in which M could be sent to arbitrarily large values, to disappear from observables after renormalization.

On the other hand we know that QCD being renormalizable has a logarithmic dependence on the ultraviolet cutoff. While this difference from the quadratic dependence on M in the truncated meson theory has been in the 1980s a subject of criticism of our approach, one should emphasize that these two dependences are not inconsistent with each other. Indeed, the strict logarithmic cutoff dependence of QCD is valid only at short distances whereas power counting supple-

mented with chiral symmetry requires quadratic dependence on the cutoff for the long-distance behavior of QCD. For high values of M, after the inclusion of vector mesons and heavier meson states, this quadratic dependence on M should smoothly turn into a logarithmic dependence as expected in the full meson theory. In fact, as demonstrated in Sect. 4, already the inclusion of vector mesons shows that this expectation is correct.

In the evaluation of the matrix elements $\langle\pi\pi|Q_i(\mu)|K\rangle$ the simplest choice one can make is $\mu = M$. This identification of μ with M is certainly an idealization in the approximate treatment used in our papers, but it can be improved with a complete description of quark–gluon and meson pictures used for short- and long-distance physics, respectively. In particular, in order to relate μ to M, one should go beyond the Fermi limit for the W-propagator and calculate at NLO the Wilson coefficients not in the usual NDR-$\overline{\text{MS}}$ scheme but in a momentum scheme. We will discuss this issue in Sect. 5. Moreover, one should go beyond the octet approximation for the light pseudoscalars by including at least the lowest-lying vector mesons. We will do it in Sect. 4.

3.2 Basic Lagrangian of the truncated meson theory

In order to calculate the hadronic matrix elements of local operators in our approach we use a truncated chiral Lagrangian describing the low-energy interactions of the lightest mesons [9,10,68]

$$L_{tr} = \frac{f_\pi^2}{4}\left[\text{Tr}(D_\mu U D_\mu U^+) + rTr(m(U+U^+)) - \frac{r}{\Lambda_\chi^2}\text{Tr}(m(D^2U + D^2U^+))\right] \tag{13}$$

where

$$U = \exp\left(i\frac{\Pi}{f_\pi}\right), \qquad \Pi = \sum_{a=1}^{8}\lambda^a\pi^a \tag{14}$$

is the unitary chiral matrix describing the octet of pseudoscalars. The singlet pseudoscalar meson η_0 decouples due to a large mass generated by the axial anomaly. In (13), $D_\mu U$ is the usual weak covariant derivative acting on the U field and m is the real and diagonal quark mass matrix. At $\mathcal{O}(p^2)$ and in the isospin limit $m_u = m_d = m_{ud}$,

$$m_\pi^2 = rm_{ud}, \quad m_K^2 = \frac{r}{2}(m_s + m_{ud}), m_8^2 = \frac{4}{3}m_K^2 - \frac{1}{3}m_\pi^2. \tag{15}$$

We would like to emphasize that the chiral Lagrangian in (13) must not be viewed as a normal effective tree Lagrangian but instead must be used as a fully interacting field theory including loop effects. In this sense we are providing a bosonization of the fundamental quark theory where all the quark currents and densities, presented below, have a valid representation in terms of the meson fields. But in the truncated version, the meson representation is valid only for a proper description of long-distance physics.

The parameter Λ_χ in (13) sets the scale of higher order terms which are always expected in a truncated theory. It should be emphasized that this scale is a hadronic scale different from Λ_{QCD}. As shown in [11,68] its value can be determined from the physical pseudoscalar masses and decay constants:

$$\Lambda_\chi^2 = F_\pi\frac{m_K^2 - m_\pi^2}{F_K - F_\pi} + \mathcal{O}\left(\frac{1}{N}\right) \Rightarrow \Lambda_\chi \approx 1.1 \text{ GeV}, \tag{16}$$

where we used the most recent lattice value for the ratio $F_K/F_\pi \approx 1.20$. The $1/N$ correction, calculated in [11], is positive and in the ballpark of 5–10 % for the range of M considered. As this correction is only logarithmically dependent on this scale, Λ_χ is practically independent of M with variation in the range $0.6 \text{ GeV} \leq M \leq 0.8 \text{ GeV}$ of less than 2 %.

As stressed in [11] this cutoff independence of Λ_χ results only if the cutoff dependence of $f_\pi(M^2)$ following from our Lagrangian is taken into account. Explicitly one finds [11]:

$$\left[f_\pi^2(M^2)\right]^P = F_\pi^2 + 2I_2\left(m_\pi^2\right) + I_2\left(m_K^2\right) \tag{17}$$

where

$$I_2(m_i^2) = \frac{i}{(2\pi)^4}\int\frac{\text{d}^4q}{q^2 - m_i^2} = \frac{1}{16\pi^2} \times\left[M^2 - m_i^2\ln\left(1 + \frac{M^2}{m_i^2}\right)\right] \tag{18}$$

results from the calculation of one-loop diagrams in Fig. 1 of [11], as signaled by the $1/16\pi^2$ factor, with M denoting the euclidean cutoff of the truncated meson theory. In this manner $1/f_\pi^2(M^2)$ is the meson picture analog of the QCD running coupling in the quark picture. In fact it is amusing to note that $1/f_\pi^2(M^2)$ decreases with increasing M implying some kind of precocious asymptotic freedom behavior:

$$\frac{\partial}{\partial M^2}\left(\frac{1}{f_\pi^2(M^2)}\right) < 0. \tag{19}$$

With the superscript P in (17), we indicate that only pseudoscalar mesons have been included. The corresponding values of $f_\pi(M^2)$ are given in the first row of Table 2.

The chiral Lagrangian (13) contains only terms with a single trace over flavor indices which reflects the large N structure of QCD. The leading N contributions to any quantity are simply obtained from the tree diagrams whereas the leading $1/N$ corrections are found by calculating the one-loop contributions. More generally, the $1/N$ expansion corresponds to the loop expansion characterized by inverse pow-

ers of $(4\pi f_\pi)^2 (f_\pi^2 \sim N)$ with the strong interaction vertices given by the truncated Lagrangian in (13). It is similar to an expansion in inverse powers of M_p^2 ($G_N = 1/M_p^2$) if one treats general relativity as an effective field theory for gravity which is modified above the Planck scale by new degrees of freedom.[4] Other details on the Lagrangian in (13) can be found in [11] and in the lecture notes [20,21].

3.3 The structure of hadronic matrix elements

The resulting matrix elements of *current–current* operators in this approach have then the structure ($i = 1, 2$)

$$\langle \pi\pi | Q_i(\mu) | K \rangle = A_i \sqrt{N} \left[1 + \frac{B_i(\mu)}{N} + \mathcal{O}\left(\frac{1}{N^2}\right) \right] \tag{20}$$

where A_i and B_i are N-independent numerical expansion coefficients which, in our approach, are given in terms of the parameters of the truncated Lagrangian. Note that the μ dependence in the matrix elements of $Q_{1,2}$ appears as a $1/N$ correction. This is consistent with the μ dependence of the Wilson coefficients $z_{1,2}(\mu)$ and reflects the simple fact that the anomalous dimensions of $Q_{1,2}$ vanish in the large N limit.

On the other hand, for *penguin* operators Q_6 and Q_8 the matrix elements have the structure ($i = 6, 8$)

$$\langle \pi\pi | Q_i(\mu) | K \rangle = \tilde{A}_i(\mu) \sqrt{N} \left[1 + \frac{\tilde{B}_i(\mu)}{N} + \mathcal{O}\left(\frac{1}{N^2}\right) \right]. \tag{21}$$

The important difference relative to (20) is the appearance of the μ dependence already in the leading term. Again, this is consistent with the μ dependence of $z_{6,8}(\mu)$ and $y_{6,8}(\mu)$ and reflects the fact that the anomalous dimensions of density–density operators do not vanish in the large N limit but are twice the anomalous dimension of the mass operator. This fact allows a better matching of the truncated meson theory with the short-distance contributions than is possible for the current–current operators in the case of $K \to \pi\pi$ amplitudes.

In order to calculate the matrix elements of the local operators in question we need meson representation of the quark currents and the quark densities. They are directly obtained from the effective Lagrangian in (13) and are given, respectively, as follows:

$$\bar{q}_L^j \gamma_\mu q_L^i = i \frac{f_\pi^2}{4} \Big\{ (\partial_\mu U) U^+ - U (\partial_\mu U^+) - \frac{r}{\Lambda_\chi^2} \left[m (\partial_\mu U^+) - (\partial_\mu U) m \right] \Big\}_{ij} \equiv (J_\mu)_{ij}, \tag{22}$$

$$\bar{q}_R^j q_L^i = -\frac{f_\pi^2}{4} r \left[U - \frac{1}{\Lambda_\chi^2} \partial^2 U \right]_{ij}. \tag{23}$$

We close the summary of our dual approach by stressing two major differences from the usual chiral perturbative calculations [1,69].

- First, the large N structure of the basic truncated low-energy Lagrangian provides a simplification over those effective Lagrangians used by chiral perturbation practitioners. In particular, within our ultraviolet quark–gluon completion, no $\mathcal{O}(p^4)$ counter-terms are needed to absorb divergences generated by a dimensional regularization.
- More importantly, our loop calculations employ a cut-off regularization and consequently our results exhibit a *quadratic* dependence on the *physical* cutoff M. This quadratic dependence is lost in the usual chiral perturbative calculations, which are based on the dimensional regularization. In effect, dimensional regularization makes extra infrared subtractions of quadratically divergent terms. These subtractions are not permitted in the full integration of the loop contributions in the truncated theory. As this quadratic dependence on the physical cutoff is usually a subject of criticism, we want to emphasize that it is an essential ingredient in the matching of the meson and quark–gluon pictures. Once again, it is required by power counting and chiral symmetry. Moreover, it stabilizes the $1/N$ expansion as exemplified through the cutoff independence of the hadronic scale Λ_χ. Last but not least, it is at the source of the $\Delta I = 1/2$ rule in our dual approach for QCD.

It is evident from these comments and from the review in [1] that in contrast to our $1/N$ approach, the chiral perturbation theory framework, while being very powerful in the determination of low-energy constants from experiment, cannot by itself address the issue of the dynamics behind the $\Delta I = 1/2$ rule and the evaluation of $\hat{B}_K$, $B_6^{(1/2)}$, and $B_8^{(3/2)}$.

With this brief formulation of our approach at hand, we are ready to summarize the most important results obtained by us in [8–12] as well as to improve them through the inclusion of vector meson contributions (Sect. 4) and the calculation of Wilson coefficients in a momentum scheme (Sect. 5) that allows a proper matching between meson and quark–gluon evolutions. Due to these improvements and the fact that several input parameters (see Table 1) are now much better known, our results are more precise than in the 1980s. We will also confront our findings with most recent lattice calculations in Sect. 9.

[4] We thank John Donoghue for pointing out this analogy.

Table 1 Values of various quantities in units of MeV discussed in the text

m_π	m_K	m_8	m_V	F_π	F_K	$m_s(0.8\ \text{GeV})$
135.0	497.6	569.3	800.0	91.8	110.4	155.0

4 Inclusion of vector mesons

4.1 Preliminaries

We will now include vector meson contributions following [21,48]. As discussed in Sect. 3.1, the matrix elements of currents and densities are described by meson tree amplitudes to leading order in the $1/N$ expansion. We have argued that the pion chiral Lagrangian can be used to compute the correct infrared behavior of these amplitudes. The vector mesons, being the next lightest states in the meson spectrum, are expected to play an important role in determining how the amplitudes evolve to higher energies. As in deep inelastic scattering and in QCD sum rules, we expect some form of local duality to determine the interplay between neighboring states and eventually generating the smooth behavior of the perturbative short-distance expansion. By constructing an effective field theory that includes smoothly the vector meson contributions we will see how this duality begins to emerge as the amplitudes evolve in energy. In the meson picture, additional heavy states will have to be added to continue this evolution and improve the matching further. We will return to this point below.

In the chiral limit, the effective Lagrangian for strongly interacting pseudoscalar Goldstone bosons

$$L(\pi) = \frac{f_\pi^2}{4}\ \text{Tr}\ \partial_\mu U \partial^\mu U^\dagger \tag{24}$$

is invariant under the *global* $SU(3)_L \times SU(3)_R$ chiral symmetry with

$$U \to g_L U g_R^\dagger. \tag{25}$$

If we define

$$U \equiv \xi\xi \tag{26}$$

then

$$\xi \to g_L \xi h^\dagger(x) = h(x) \xi g_R^\dagger, \tag{27}$$

with $h(x)$ any 3×3 unitary transformation, turns out to be a *local* symmetry of this Lagrangian. We may thus introduce the low-lying nonet V of vector mesons as the gauge bosons of this hidden $U(3)$ symmetry [70] by imposing the following transformation law:

$$V \to \frac{i}{g} h \partial_\mu h^\dagger + h V h^\dagger. \tag{28}$$

In this manner, the effective Lagrangian becomes

$$L(\pi, V) = L(\pi) - \frac{1}{4}\ \text{Tr}\ V_{\mu\nu} V^{\mu\nu} - a\frac{f_\pi^2}{4}\ \text{Tr}\ \{\partial_\mu \xi^\dagger \xi + \partial_\mu \xi \xi^\dagger - 2ig V_\mu\}^2. \tag{29}$$

In the absence of the standard non-abelian field-strength $V_{\mu\nu}$, the vector mesons would not propagate but just be auxiliary fields such that $L(\pi, V)$ consistently reduces to $L(\pi)$ whatever the value of the free parameter a associated with the averaged $V_\mu V^\mu$ mass term. In the presence of a kinetic term for the vector mesons, they become dynamical and their low-energy properties are nicely reproduced if $a \cong 2$.

At this point it is useful to stress the difference between the treatment of vector bosons in our approach and in the usual chiral perturbation theory. It is well known that in the latter approach the introduction of massive spin-1 particles (such as vector mesons) in an effective Lagrangian carries some model dependence. But in the context of estimating the $\mathcal{O}(p^4)$ chiral low-energy constants these ambiguities can be removed provided all the models of spin-1 resonances respect certain QCD asymptotic constraints [71].

In our dual approach, as already stressed in the previous section, we do not have to worry about $\mathcal{O}(p^4)$ chiral low-energy constants as they are part of the quark–gluon evolution which satisfies the QCD asymptotic constraints. For illustration, in [72], we have explicitly shown that the "hidden-symmetry" approach and the "massive Yang–Mills" approach are equivalent, leading both to (33) for the $\pi^+ - \pi^0$ mass difference discussed below.

We will now demonstrate how the matching between the *meson evolution* and the *quark–gluon evolution* is significantly improved through the inclusion of the nonet of light vectors in our truncated meson theory [21]. In the chiral limit, they all have a mass m_V around 0.8 GeV and their one-loop contributions tend to transmute the quadratic cutoff dependence of weak hadronic matrix elements into logarithmic one.

In this matching context, when performing the quark–gluon evolution down to $\mu = (0.8\text{–}1.0)$ GeV we should consider all the $q\bar{q}$ resonances around this scale. In this spirit, the 1^{--} vector nonet $(\omega - \phi, \rho, K^*)$ with masses in the range (0.77–1.02) GeV has to be included. The next, well-identified 1^{+-} axial-vector nonet (f_1, a_1, K_1) has masses in the ballpark of (1.23–1.43) GeV, that is, well above the matching scales we consider. It plays a non-negligible role in the estimate of the $\pi^+ - \pi^0$ mass difference discussed below as indicated in (33). On the other hand as demonstrated in [21,48] it is by far less important for $\hat{B}_K$. While it would be interesting to include these higher resonances in order to see the quadratic behavior in the physical cutoff M turning into a logarithmic one, from the present perspective the

increased number of parameters in the corresponding effective Lagrangian relative to the one in (29) does not allow us to expect an improved precision of our approach through the inclusion of these resonances. These parameters are associated with the averaged $V_\mu V^\mu$ vector mass term, $A_\mu A^\mu$ axial-vector mass term and $A_\mu \partial^\mu \pi$ mixing term. Future lattice simulations, if performed at $\mathcal{O}(1\ \text{GeV})$ scale, should be able to shed more light at this issue.

4.2 $f_\pi(M^2)$

In the chiral model defined by (29), the lowest-lying pseudoscalars are massless and the tree-level pion decay constant is modified by one-loop meson corrections in the following way [21]:

$$f_\pi^2(M^2) = F_\pi^2 + \frac{3}{16\pi^2}\left\{\left(1-\frac{9a}{16}\right)M^2 + \frac{9a}{16}m_V^2 \ln\left(1+\frac{M^2}{m_V^2}\right)\right\}. \tag{30}$$

In the decoupling limit $m_V \gg M$, we consistently recover the quadratic M-dependence in (17), whatever the value of a. But for $a = 16/9$, this quadratic dependence on the cutoff would totally disappear in favor of the logarithmic one.

Combining then (17) and (30) with the realistic values $m_{\pi,K}^2 \neq 0$ and $a = 2$, respectively, we arrive at the expression

$$\left[f_\pi^2(M^2)\right]^{P+V} = \left[f_\pi^2(M^2)\right]^P + \Delta\left[f_\pi^2(M^2)\right]^V \tag{31}$$

where

$$\Delta\left[f_\pi^2(M^2)\right]^V = -\frac{27}{8}I_2(m_V^2) \tag{32}$$

with the function I_2 defined in (18).

As seen in Table 2 the dependence of f_π on M is now much weaker since the logarithmic terms dominate now the meson evolution of $f_\pi(M^2)$.

Although expected from the dual representation of the strong dynamics for large N, such transmutation of the quadratic cutoff dependence in favor of a logarithmic one reminds us of the $\pi^+ - \pi^0$ (squared) mass splitting where a similar one-loop calculation including both the vector and the axial-vector mesons gives

Table 2 The anatomy of $f_\pi(M^2)$. P and V indicate that pseudoscalar and vector mesons have been included or left out

$M = \mu$ (GeV)	0.6	0.7	0.8	0.9	1.0	Comments
$f_\pi(M^2)$ (MeV)	114.7	123.5	133.3	143.7	154.8	(P)
$f_\pi(M^2)$ (MeV)	107.6	112.1	116.4	120.6	124.3	(P + V)

$$\Delta m^2(0^{-+}, 1^{--}, 1^{++}) = \left(\frac{3}{4\pi}\right)\alpha_{\text{QED}}\int_0^{M^2} \mathrm{d}q^2 \frac{(m_V m_A)^2}{(q^2+m_V^2)(q^2+m_A^2)} \tag{33}$$

in agreement with the quark–gluon contribution for large q^2 (i.e., $q^2 \gg m_{V,A}^2$) [21,72]:

$$\Delta m^2(\text{quark}-\text{gluon}) = \left(\frac{3}{4\pi}\right)\alpha_{\text{QED}}F_\pi^2(\alpha_s r^2)\int_{M^2}^{\infty}\frac{\mathrm{d}q^2}{q^4}, \tag{34}$$

where r is the parameter in (13).

In this one-loop calculation, the identification of the momentum for the virtual quarks and gluons with the momentum for the virtual mesons is straightforward since they are the same as the one carried by the color-singlet photon. So, we are able to keep track of the momentum flow and work in the chiral SU(2) limit for both the quark–gluon and the meson evolutions. But here, again, we record that the meson theory truncated to the massless pseudoscalars leads to a pure quadratic dependence on the physical cutoff:

$$\Delta m^2(0^{-+}) = \left(\frac{3}{4\pi}\right)\alpha_{\text{QED}}M^2 \tag{35}$$

for small q^2 (i.e., $q^2 \ll m_{V,A}^2$). In other words, if the ultraviolet completion for the truncated π-meson theory was not yet known, the observed $\pi^+ - \pi^0$ electromagnetic mass splitting would then be explained by the existence of new degrees of freedom around the cutoff $M \approx 0.85$ GeV.

4.3 $J_\mu \otimes J^\mu(M^2)$

A similar though not so striking transmutation occurs for the left-handed current–current operators in the chiral model defined in (29):

$$\{(J_\mu)_{ij}(J^\mu)_{kl}\}(M^2) = \{(\bar{J}_\mu)_{ij}(\bar{J}^\mu)_{kl}\}(0) - c(M^2)\{(J_\mu)_{il}(J^\mu)_{kj} - \frac{1}{2}[\delta_{il}(J_\mu J^\mu)_{kj} + \delta_{kj}(J_\mu J^\mu)_{il}]\}(0) \tag{36}$$

with $(J_\mu)_{ij}$ defined in (22) and

$$\bar{J}_\mu = i\frac{F_{\pi,K}}{2}\partial_\mu\pi + \frac{i}{4}[(\partial_\mu\pi)\pi - \pi(\partial_\mu\pi)] + \cdots \tag{37}$$

being the relevant $\Delta S = 0, \pm 1$ physical hadronic current. Moreover

$$c(M^2) = \frac{1}{16\pi^2}\left[\frac{2M^2}{f^2}\right] + \frac{3a}{16f^2} \times \left\{(a-5)I_2\left(m_V^2\right) + am_V^2 I_3\left(m_V^2\right)\right\}, \tag{38}$$

where the function $I_3(m_i^2)$ is just the derivative of $I_2(m_i^2)$ with respect to m_i^2

$$I_3(m_i^2) \equiv \frac{dI_2(m_i^2)}{dm_i^2} = \frac{1}{16\pi^2} \times \left[\frac{M^2}{M^2+m_i^2} - \ln\left(1+\frac{M^2}{m_i^2}\right)\right]. \quad (39)$$

For ($m_V \to \infty$, a arbitrary) and ($a \to 0$, m_V arbitrary) only the first term on the r.h.s. of (38) survives, corresponding precisely to the pseudoscalar contribution in the chiral limit.

5 Matching of meson and quark–gluon evolutions

The identification of M and μ has been the subject of criticism in the past. Therefore we would like to discuss this point and present an improved treatment that goes beyond our work of 1980s. First, as discussed in particular in [18,22,23] and [73], in the large N expansion the non-factorized amplitudes responsible for both meson and quark–gluon evolutions are given by a convolution of the W-boson propagator $D_W^{\mu\nu}(q)$ with a tree amplitude $A_{\mu\nu}$ as follows:

$$A(p_1,..p_n) = i\int \frac{\mathrm{d}^4q}{(2\pi)^4} D_W^{\mu\nu}(q) A_{\mu\nu}(q,p_1,..p_n). \quad (40)$$

The short- and long-distance contributions to this amplitude are controlled by the explicit momentum flowing through the W-boson propagator. These contributions can be separated by a suitable regularization of this integration. An explicit example is provided by the analytic regularization

$$D_W^{\mu\nu}(q) \to D_W^{\mu\nu}(q)\left[\frac{q^2}{q^2-M^2} + \frac{-M^2}{q^2-M^2}\right], \quad (41)$$

which we will use in what follows. The first term contributes at short distances but is suppressed at low momentum. The second term contributes at long distances but the high momentum components are suppressed. This separation can be exploited to use the quark–gluon representation for the first term and a truncated meson Lagrangian for the second term.

Now, it is well known that the Wilson coefficients depend on renormalization scheme and are usually computed using dimensional regularization for UV and various schemes for γ_5 in D dimensions like NDR or HV schemes [74]. In order to be able to make the identification

$$(M^2)_{\text{mesons}} = (\mu^2)_{\text{quark-gluon}}, \quad (42)$$

we have to relate the Wilson coefficients calculated in these schemes to the ones in which the integral in (40) is calculated in $D = 4$ with an UV momentum cutoff. We call this scheme $\overline{\text{MOM}}$ scheme. The *bar* indicates that this scheme should not be confused with momentum schemes used in the past for short-distance calculations.

This shift in Wilson coefficients can be found as usual by calculating perturbatively in the quark–gluon picture one-loop matrix elements of operators in different schemes for UV but using the same IR regulator and comparing the finite non-logarithmic pieces. In the case at hand, retaining only the first term in (41) and setting the external momenta to be zero corresponds effectively to regulating IR divergences by giving the mass M to the gluon. Proceeding in this manner the coefficients z_1 and z_2 in the $\overline{\text{MOM}}$ scheme to be combined with the meson evolution can be obtained from the known coefficients calculated in the NDR-$\overline{\text{MS}}$ scheme. Details can be found in [23], where the same results for the $\overline{\text{MOM}}$ scheme have been obtained calculating the shift relative to the HV scheme. One finds then

$$z_1(\overline{\text{MOM}}) = z_1(\text{NDR}) + \frac{\alpha_s}{4\pi}\frac{11}{2N} z_1(\text{NDR}) - \frac{\alpha_s}{4\pi}\frac{11}{2} z_2(\text{NDR}), \quad (43)$$

$$z_2(\overline{\text{MOM}}) = z_2(\text{NDR}) - \frac{\alpha_s}{4\pi}\frac{11}{2} z_1(\text{NDR}) + \frac{\alpha_s}{4\pi}\frac{11}{2N} z_2(\text{NDR}). \quad (44)$$

These results have been confirmed in the present paper.

As the matrix elements of Q_6 operator are presently known only in the large N limit, it is sufficient to use for z_6 coefficient only its LO result that is in any case $\mathcal{O}(1/N)$ and, moreover, GIM suppressed. To this end we will use α_s given in the $\overline{\text{MS}}$ scheme and the known leading order anomalous dimensions.

The results for z_1, z_2 in $\overline{\text{MOM}}$ and NDR schemes for different μ are given in Table 3. We observe large enhancement of $|z_{1,2}|$ in the momentum scheme over the values in the NDR scheme. We have checked that for the same value of the coupling constant the leading order values of $z_{1,2}$ are between those obtained in $\overline{\text{MOM}}$ and NDR schemes.

In order to complete the matching we have to calculate the relevant loop diagrams in the meson theory, including in

Table 3 Values of the Wilson coefficients z_i as functions of μ for the $\overline{\text{MOM}}$ and NDR-$\overline{\text{MS}}$ schemes

μ (GeV)	0.6	0.7	0.8	0.9	1.0	Comments
$\alpha_s(\mu)$	0.812	0.658	0.564	0.502	0.457	$\overline{\text{MS}}$
$z_1(\mu)$	−1.228	−1.029	−0.900	−0.809	−0.740	$\overline{\text{MOM}}$
$z_2(\mu)$	1.777	1.625	1.530	1.463	1.415	$\overline{\text{MOM}}$
$z_6(\mu)$	−0.069	−0.049	−0.037	−0.029	−0.023	LO
$z_1(\mu)$	−0.660	−0.590	−0.537	−0.495	−0.461	NDR-$\overline{\text{MS}}$
$z_2(\mu)$	1.379	1.328	1.291	1.262	1.240	NDR-$\overline{\text{MS}}$
$z_6(\mu)$	−0.097	−0.065	−0.047	−0.035	−0.027	NDR-$\overline{\text{MS}}$

the integrands the second term in (41). We find then a simple rule for transforming the results of our previous papers into the ones obtained using an analytic regularization that can be properly combined with the coefficients z_i in $\overline{\text{MOM}}$ scheme. One just has to replace the function $I_2(m_i^2)$ in (18) by[5]

$$\hat{I}_2(m_i^2) = \frac{i}{(2\pi)^4}\int \frac{\mathrm{d}^4 q}{q^2-m_i^2}\left[\frac{-M^2}{q^2-M^2}\right] = \frac{1}{16\pi^2}\frac{M^2}{M^2-m_i^2}\left[\ln(2)M^2 - m_i^2\ln\left(1+\frac{M^2}{m_i^2}\right)\right] \tag{45}$$

with the limiting value for $M^2 = m_V^2$

$$\hat{I}_2(m_V^2) = \frac{1}{16\pi^2}m_V^2\left[\ln(2)-\frac{1}{2}\right]. \tag{46}$$

Similarly, the function $I_3(m_i^2)$ in (39) should be replaced by the derivative of $\hat{I}_2(m_i^2)$ in (45). We find then

$$\hat{I}_3(m_i^2) = \frac{1}{16\pi^2}\frac{M^4}{(M^2-m_i^2)^2} \times\left[\ln(2)+\frac{M^2-m_i^2}{M^2+m_i^2}-\ln\left(1+\frac{M^2}{m_i^2}\right)\right] \tag{47}$$

and the limiting value for $M^2 = m_V^2$

$$\hat{I}_3(m_V^2) = -\frac{1}{16\pi^2}\left[\frac{1}{8}\right]. \tag{48}$$

It should be noted that the presence of ln(2) multiplying M^2 will in turn decrease in the $\overline{\text{MOM}}$ scheme the matrix elements relative to our previous results, while as we have seen above in the $\overline{\text{MOM}}$ scheme $|z_{1,2}|$ become consistently larger than in the LO.

6 The parameter $\hat{B}_K$

6.1 Preliminaries

As the physics behind the $\Delta I = 1/2$ rule is more involved than the one in K^0–$\bar{K}^0$ mixing, it is strategically useful to apply first our approach to the calculation of the parameter $\hat{B}_K$. We will first only include pseudoscalar meson contributions, but subsequently also vector meson contributions will be taken into account. This will demonstrate explicitly that the inclusion of vector mesons significantly improves the matching between the meson and quark–gluon pictures.

[5] Needless to say this replacement should not be made in the calculation of f_π, where no meson evolution is involved.

The renormalization group invariant parameter is given as follows [75]:

$$\hat{B}_K = B_K(\mu)\left[\alpha_s^{(3)}(\mu)\right]^{-b}\left[1+\frac{\alpha_s^{(3)}(\mu)}{4\pi}J_3\right], \quad b = \frac{9(N-1)}{N(11N-6)}, \tag{49}$$

where we have shown the N-dependence of the exponent b in the leading term to signal that b vanishes in the large N limit. The coefficient J_3 is renormalization scheme dependent. It has been calculated in the NDR-$\overline{\text{MS}}$ in [75]. However, as discussed in the previous section, in our approach we have to work in a $\overline{\text{MOM}}$ scheme.

As the operator $\Delta S = 2$ and the $\Delta I = 3/2$ operator have the same anomalous dimension, relations in (43) and (44) allow us to calculate the shift in J_3 entering $\hat{B}_K$ in (49). From the $\mathcal{O}(\alpha_s)$ term in the sum $z_1 + z_2$ we obtain

$$J_3(\overline{\text{MOM}}) = J_3(\text{NDR}) - \frac{11}{2}\left(1-\frac{1}{N}\right). \tag{50}$$

Using the known NDR result from [75] and setting $N = 3$ we find

$$J_3 = 1.895\ (\text{NDR}), \qquad J_3 = -1.772\ (\overline{\text{MOM}}). \tag{51}$$

The scale dependent parameters $B_K(\mu)$ is related to the relevant hadronic matrix element of the $\Delta S = 2$ operator

$$Q(\Delta S = 2) = 4(\bar{s}_L\gamma^\mu d_L)(\bar{s}_L\gamma_\mu d_L) \tag{52}$$

as follows:

$$\langle\bar{K}^0|Q(\mu)|K^0\rangle = B_K(\mu)\frac{16}{3}F_K^2 m_K^2. \tag{53}$$

The normalization of B_K is such that in the vacuum insertion approximation B_K is unity. Indeed

$$B_K(\mu) = \frac{3}{4}\left(1+\frac{1}{N}\right) = 1, \qquad (\text{in VIA}) \tag{54}$$

where the $1/N$ represents again the Fierz term. As already stressed in [12], this term completely misrepresents the full $1/N$ correction to the leading term. Its positive sign as opposed to the negative sign required for the matching with $1/N$ corrections in the quark–gluon evolution and the absence of any μ dependence in this result show that it is incompatible with the quark–gluon picture of QCD. This has been recently confirmed in lattice QCD [44].

On the other hand, the leading term of $B_K = 3/4$ [8, 54] is the correct prediction of truncated meson theory in the strict large N limit. Indeed, at this stage the following important point should be made. As in the strict large N limit the exponent in (49) and the NLO term involving J_3 vanish, we find that independently of any renormalization scale or renormalization scheme for the operator $Q(\Delta S = 2)$ in the large N limit

$$\hat{B}_K \to 0.75, \qquad \text{(in large N limit)}. \tag{55}$$

The question then arises whether after the inclusion of $1/N$ corrections $\hat{B}_K$ is larger or smaller than its leading value. In the 1980s the values of $\hat{B}_K$ varied from 1/3 obtained using PCAC-SU(3) [76], 0.40 obtained through hadronic sum rules [77] to values close to unity, obtained in particular within the lattice approach [45]. On the other hand, using the truncated meson theory outlined in Sect. 3 and thereby including only pseudoscalar meson contributions we have found $1/N$ corrections to be small and *negative*. However, the left-over albeit weak μ dependence of $\hat{B}_K$ and the inaccurate value of α_s at that time lead us to a rather conservative error on $\hat{B}_K$ [12]

$$\hat{B}_K = 0.66 \pm 0.07, \qquad \text{(in dual QCD, 1987)}. \tag{56}$$

Shortly after, it has been shown that the inclusion of vector mesons in this calculations [21,48] moved $\hat{B}_K$ much closer to its leading order value in (55). Since then several semi-analytic calculations by other authors have been performed. They are reviewed in [1].

On the other hand, a quarter of century after our first result the world lattice average for $\hat{B}_K$ based on the calculations of various groups [78–83] reads for $N_f = 2 + 1$ calculations (recent FLAG update of [81])

$$\hat{B}_K = 0.766 \pm 0.010, \qquad \text{(in lattice QCD, 2013)}. \tag{57}$$

See also the very recent analyses in [84–86]. The following remarks are in order

- The precision of lattice result is truly impressive, though on the verge of being challenged by isospin breaking effects.
- The value in (57) is consistent with our estimate in (56) which we will update below. Moreover, it is very close to the leading N result in (55).
- The sign of the correction to leading N result obtained presently in the lattice calculations appears to be *positive* and not *negative* as favored in our framework and discussed below.

After recalling the analytic expressions for $\hat{B}_K$ in the truncated meson theory and including vector meson contributions, we will give arguments in favor of a *negative* correction to the leading large N result so that in QCD we expect:

$$\hat{B}_K \leq 0.75, \qquad \text{(in 1/N expansion)}. \tag{58}$$

Therefore we believe that the lattice error in (57) is underestimated and the improved lattice calculations will satisfy the bound in (58) giving values for $\hat{B}_K$ a bit lower than the present world lattice average. In fact, a number of lattice groups among [78–83] published results with central values satisfying the bound in (58) but the errors did not allow for a clear cut conclusion.

6.2 Calculating $\hat{B}_K$ in the truncated meson theory

Including one-loop contributions in the meson theory truncated to pseudoscalar mesons as done in [12] and performing the replacements (45) and (47), we find

$$B_K^P(M) = \frac{3}{4}\left\{1 - \frac{1}{4F_K^2}\left[3\left(1+\frac{m_8^2}{m_K^2}\right)\hat{I}_2\left(m_8^2\right) + \left(1+\frac{m_\pi^2}{m_K^2}\right)\hat{I}_2\left(m_\pi^2\right) + 4m_K^2\hat{I}_3\left(m_K^2\right)\right]\right\}. \tag{59}$$

With the superscript P we indicate that only pseudoscalar mesons have been included.

In Table 4 we give $B_K(\mu)$ and $\hat{B}_K$ obtained using (49) and (59) with $\mu = M$. We confirm that while $B_K(\mu)$ depends strongly on μ, this μ dependence is canceled significantly by the μ dependent factor coming from the QCD analysis in the quark–gluon picture. On a semi-quantitative level this reduction of μ dependence shows that the quark–gluon and the meson pictures of strong interactions match well as required for the consistency of our calculation. Yet, for M = (0.6–0.7) GeV the accuracy of the μ dependent factor coming from the quark–gluon picture cannot be trusted as in this range $\alpha_s(\mu) \geq 0.65$. On the other hand, for $M \geq 0.8$ GeV, $\hat{B}_K$ shows a significant M dependence signaling that the meson evolution described by means of pseudoscalars only ceases to be a good approximation. Therefore in order to decrease the gap between the validity of both pictures, the inclusion of vector mesons is necessary. Yet, already at this stage we note two facts

- $B_K^P(M)$ given here in the $\overline{\text{MOM}}$ scheme differs significantly from the values quoted by lattice groups that use the NDR-MS scheme. In the latter scheme the values of this parameter are much lower.
- However, this difference is compensated by the QCD factor in (49) being significantly above unity in the NDR-$\overline{\text{MS}}$ scheme, while it is close to unity in the $\overline{\text{MOM}}$ scheme. Indeed the LO enhancement of this factor present in any scheme is significantly compensated by the negative NLO correction in the $\overline{\text{MOM}}$ scheme as seen in (51).

Table 4 The anatomy of B_K as a function of the scale M

M (GeV)	0.6	0.7	0.8	0.9	1.0	Comments
$B_K^P(M)$	0.698	0.665	0.622	0.568	0.502	(P)
$\hat{B}_K^P$	0.647	0.662	0.650	0.615	0.559	
$B_K(M)$	0.728	0.716	0.700	0.679	0.653	(P + V)
$\hat{B}_K$	0.676	0.713	0.731	0.735	0.728	

It should be noted that in the chiral limit, $m^2_{\pi,K} \to 0$, the result in (59) implies

$$B_K(M) = \frac{3}{4}\left(1 - \frac{2M^2}{(4\pi F_K)^2}\right), \tag{60}$$

so that for $M = 0.7$ GeV one finds $B_K(M) = 0.37$. As seen in Table 4 this strong suppression is significantly softened for $m^2_{\pi,K} \neq 0$, see also [29], but on the whole the resulting value of $\hat{B}_K$ is visibly below the lattice value in (57). As we will now demonstrate, after the inclusion of vector contributions, the final result for $\hat{B}_K$ will turn out to be very close to the lattice result.

6.3 Inclusion of vector meson contributions in $\hat{B}_K$

From the generic formula (36), one easily infers how the inclusion of the lowest-lying vector mesons modifies the cutoff dependence of the B_K parameter. In the chiral limit and for $a = 2$ one has [21,48]

$$B_K(M) = \frac{3}{4}\left\{1 - \frac{1}{(4\pi F_K)^2}\left[\frac{7}{8}M^2 + \frac{3}{8}m_V^2 \ln\left(1 + \frac{M^2}{m_V^2}\right) + \frac{3}{4}\frac{m_V^2 M^2}{(M^2 + m_V^2)}\right]\right\}. \tag{61}$$

In the decoupling limit $m_V \gg M$, we consistently recover the result in (60). But for $M > m_V$, we observe a reduction by more than 50 % of the quadratic dependence on the cutoff. Once again, this transmutation of the quadratic cutoff dependence in favor of a logarithmic one with the same sign is clearly linked to the introduction of a new intrinsic scale m_V which changes the power counting in a way still consistent with chiral symmetry.

Again, as in the case of pseudoscalar contributions, we have to adjust the result in (61) to the $\overline{\text{MOM}}$ scheme by means of the procedure summarized in Sect. 5. Combining then (59) and (61) properly modified by this procedure and taking into account that the contribution (60) is already present in (59), we arrive at the expression

$$B_K^{\text{tot}}(M) = B_K^P(M) + \Delta B_K^V(M) \tag{62}$$

where

$$\Delta B_K^V(M) = \frac{3}{(4F_K)^2}\left[\frac{9}{2}\hat{I}_2(m_V^2) - 3m_V^2\hat{I}_3(m_V^2)\right] \tag{63}$$

with the functions $\hat{I}_2$ and $\hat{I}_3$ defined in (45) and (47), respectively.

In Table 4 we show the results obtained using (62). The effect of the reduction of μ dependence in $\hat{B}_K$ is very significant when compared with the pseudoscalar case, again demonstrating that our evolution picture is correct. This is in particular the case in the range $M = (0.7\text{–}0.9)$ GeV where we expect our truncated meson theory after the inclusion of vector mesons to give reliable results.

We note that the effect of inclusion of vector meson has only a small impact at $M = 0.6$ GeV but this impact increases quickly with increasing M. In particular, the value of $\hat{B}_K$ is increased and turns out to be close to its leading value as the vector meson contributions enter with the opposite sign to the pseudoscalar meson contributions. On the basis of these results we quote our final result

$$\hat{B}_K = 0.73 \pm 0.02, \tag{64}$$

where the error should not be considered as a standard deviation. Rather, this result represents the range for $\hat{B}_K$ we expect in our approach. The lower value corresponds to the value at $M = 0.7$ GeV which should be sufficiently large so that our calculation is reliable and the upper bound is just the bound in (58) to which we will return below. We consider this range as conservative as the M dependence of $\hat{B}_K$ displayed in Table 4 amounts for $M = (0.8\text{–}1.0)$ GeV to only 1 %.

This result is in an excellent agreement with the lattice QCD value in (57) although we are aware of the fact that while lattice calculations have good control over their errors, this is not quite the case here. Still it is encouraging that such a simple analytic approach could provide the explanation why the lattice results turn out to be so close to the strict large N limit value of $\hat{B}_K$.

In summary, we observe that within our approach the smallness of $1/N$ corrections to the leading result for $\hat{B}_K$ follows from an approximate cancelation between pseudoscalar and vector meson one-loop contributions. Moreover, this cancelation is consistent with the small anomalous dimension of the $\Delta S = 2$ operator and consequently allows a good matching of meson and quark–gluon evolutions.

Finally, we would like to refer to the analysis in [29] which was done in the spirit of our approach except that for the low-energy meson contributions an extended Nambu–Jona-Lasinio model has been used. Moreover, a sharper matching between long-distance and short-distance contributions has been performed at the LO level in α_s. The result $0.60 \leq \hat{B}_K \leq 0.80$, even if less precise, is fully consistent with the values obtained in our approach.

6.4 An upper bound on $\hat{B}_K$

Let us next discuss the sign of $1/N$ corrections to the leading result in (55). In fact, the existence of the upper bound on the $\hat{B}_K$ parameter in (58) has been demonstrated in [46] and we recall briefly the main arguments here. To derive this bound, let us exchange a fictitious color-singlet boson between the two left-handed currents of the $\Delta S = 2$ operator in (52). In the $1/N$ expansion, the full leading and next-to-leading contributions to B_K can then be viewed as two-bubble and one-bubble topologies, respectively (see Fig. 2 of [46]). In this

simple pictorial approach, the $1/N$ Fierz term is clearly part of the second disconnected topology. For each closed quark loop (wherein the sum over all planar gluons is understood), we take indeed the trace over colors. But for each closed fermion loop, we also have to multiply by the spin-statistics factor (-1). This results in a negative $1/N$ correction to the leading value of the B_K parameter.

As seen in Table 4 our results for $\hat{B}_K$ satisfy the upper bound in question. On the other hand, the central value of $\hat{B}_K$ from lattice simulations in (57) violates this bound but is consistent within 2σ. We expect therefore that improved lattice calculations will satisfy our bound one day and in a few years from now lattice researchers will quote $\hat{B}_K \approx 0.74$. In fact, the most recent update from staggered quarks [84,86] quotes precisely $\hat{B}_K = 0.738 \pm 0.005$ but additional systematic error of 0.037 does not allow for definite conclusions.

7 ReA_0 and ReA_2 amplitudes

7.1 Preliminaries

The amplitudes for $K \to \pi\pi$, neglecting the $\Delta I = 5/2$ contributions, can be parametrized in terms of isospin amplitudes A_I through [1]

$$A(K^+ \to \pi^+\pi^0) = \frac{3}{2} A_2 e^{i\delta_2} \tag{65}$$

$$A(K^0 \to \pi^+\pi^-) = A_0 e^{i\delta_0} + \sqrt{\frac{1}{2}} A_2 e^{i\delta_2} \tag{66}$$

$$A(K^0 \to \pi^0\pi^0) = A_0 e^{i\delta_0} - \sqrt{2} A_2 e^{i\delta_2}\,. \tag{67}$$

Here the subscript $I = 0, 2$ denotes states with isospin 0, 2 equivalent to $\Delta I = 1/2$ and $\Delta I = 3/2$ transitions, respectively, and $\delta_{0,2}$ are the corresponding strong phases. The weak CKM phases are contained in A_0 and A_2. The experimental values of these amplitudes are given in the isospin limit in (1). The strong phases $\delta_{0,2}$ cannot be calculated in our framework since the $\pi\pi$ elastic rescattering has no ultraviolet completion. Their difference is measured to be [2]

$$\delta_0 - \delta_2 = (47.5 \pm 0.9)^\circ. \tag{68}$$

Equivalently, we have

$$A_0 e^{i\delta_0} = \frac{1}{3}\Big[2A(K^0 \to \pi^+\pi^-) + A(K^0 \to \pi^0\pi^0)\Big], \tag{69}$$

$$A_2 e^{i\delta_2} = \frac{\sqrt{2}}{3}\Big[A(K^0 \to \pi^+\pi^-) - A(K^0 \to \pi^0\pi^0)\Big], \tag{70}$$

where we use the following isospin relation:

$$A(K^0 \to \pi^+\pi^-) - A(K^0 \to \pi^0\pi^0) = \sqrt{2} A(K^+ \to \pi^+\pi^0) \tag{71}$$

which provides a consistency check when extracting all non-vanishing hadronic matrix elements.

7.2 Meson evolution of current–current operators

In the limit $m_\pi^2 \to 0$, the four $K \to \pi\pi$ one-loop diagrams given in Fig. 2 of [11] can be viewed as a meson operator evolution down to the factorization scale:

$$Q_1(M^2) = Q_1(0) - c_1(M^2) Q_2(0) \tag{72}$$

$$Q_2(M^2) = Q_2(0) - c_1(M^2) Q_1(0) + c_2(M^2)[Q_2(0) - Q_1(0)]. \tag{73}$$

with *positive* coefficients

$$c_1(M^2) \approx \frac{1}{(4\pi f_\pi)^2}\left[\frac{f_\pi}{F_\pi}\right]\left\{2\hat{M}^2 - \frac{m_K^2}{4}\ln\left(1 + \frac{M^2}{\tilde{m}^2}\right)\right\}, \tag{74}$$

$$c_2(M^2) \approx \frac{1}{(4\pi f_\pi)^2}\left[\frac{f_\pi}{F_\pi}\right]\left\{\hat{M}^2 + m_K^2\ln\left(1 + \frac{M^2}{\tilde{m}^2}\right)\right\}, \tag{75}$$

where the M^2 dependence of the expansion parameter f_π, given in (17), has not been written explicitly. These evolution equations, the positivity of the coefficients c_i and the fact that $c_i = \mathcal{O}(1/N)$ are fundamental for our explanation of the $\Delta I = 1/2$ rule. It originates in the continuation of the usual quark–gluon evolution by means of meson evolution below scales $\mathcal{O}(1)$ GeV down to factorization scale at which QCD becomes a theory of free interacting mesons. In what follows we want to have a closer look at these equations in order to demonstrate that they have the structure of the known renormalization group equations in (12).

The coefficients $c_i(M^2)$ in (74) and (75) include only pseudoscalar meson contributions. We will include vector meson contributions soon. The replacement of the leading M^2 dependence by

$$\hat{M}^2 = \ln(2) M^2 \tag{76}$$

in our previous papers follows from the replacement of $I_{2,3}$ by $\hat{I}_{2,3}$ in the chiral limit and allows us to combine within a very good approximation these results with z_i in the $\overline{\text{MOM}}$ scheme. The argument of the logarithmic terms is only an approximation since the mass scale $\tilde{m}$ replaces a rather complicated dependence of the exact expressions on the meson masses: $m_\pi \le \tilde{m} \le m_K$. As in our 1986 analysis we set

$$\tilde{m} = 0.3 \text{ GeV}, \tag{77}$$

although our results are not very sensitive to this choice unless $\tilde{m}$ is approaching m_π. In fact it turns out that the matching between quark–gluon and meson evolutions is best for this value. The numerical values of $c_{1,2}(M^2)$ for $M = (0.6$–$1.0)$ GeV resulting from (74) and (75) are given in Table 5.

Table 5 Values of $c_{1,2}$ as functions of M. P and V indicate whether pseudoscalar and vector mesons have been included or left out

M (GeV)	0.6	0.7	0.8	0.9	1.0	Comments
$c_1(M^2)$	0.240	0.315	0.392	0.471	0.549	(P)
$c_1(M^2)$	0.206	0.267	0.331	0.398	0.468	(P + V)
$1-c_1(M^2)$	0.760	0.685	0.608	0.529	0.451	(P)
$1-c_1(M^2)$	0.794	0.733	0.669	0.602	0.532	(P + V)
$c_2(M^2)$	0.390	0.447	0.498	0.543	0.584	(P)
$c_2(M^2)$	0.390	0.453	0.511	0.566	0.619	(P + V)

In (72) and (73), $Q_{1,2}(0)$ denote the hadronized $\Delta S = 1$ operators at the factorization scale now defined by $\mu = 0$. As a consequence, the only non-vanishing hadronic matrix elements of current–current operators for the $K \to \pi\pi$ decay amplitudes at $\mu = 0$ are

$$\langle \pi^+\pi^-|Q_2(0)|K^0\rangle = -\langle \pi^0\pi^0|Q_1(0)|K^0\rangle = X_F, \tag{78}$$

$$\langle \pi^+\pi^0|Q_1(0)|K^+\rangle = \langle \pi^+\pi^0|Q_2(0)|K^+\rangle = \frac{X_F}{\sqrt{2}}, \tag{79}$$

where

$$X_F = \sqrt{2}F_\pi\left(m_K^2 - m_\pi^2\right) \tag{80}$$

with the subscript F standing for factorization. Here we keep $m_\pi \neq 0$ as the limit $m_\pi \to 0$ is used only for operator evolution. Note that these leading hadronic matrix elements do *not* include the usual Fierz terms that are a part of non-factorizable loop corrections.

The inclusion of the $\mathcal{O}(1/N)$ non-factorizable loop corrections, represented by the non-vanishing coefficients c_i, can be viewed as taking into account the physics contributions in the momentum range from $\mu = 0$ to $\mu = M$. This is complementary to the usual renormalization group evolution for the Wilson coefficients z_i taking into account the physics contributions from $\mu = M$ to $\mu = M_W$. In this manner, all physics contributions to the amplitudes $\mathrm{Re}A_0$ and $\mathrm{Re}A_2$ from the momentum range from $\mu = 0$ to $\mu = M_W$ are included. The inferred pattern for the $Q_{1,2}$ meson evolution has been confirmed by a background field method [73] acting directly at the operator level.

The numerical implications of these results for $\mathrm{Re}A_0$ and $\mathrm{Re}A_2$ will be discussed in Sect. 8 but already now we can verify that the structure of (72) and (73) allows a plausible matching of the meson and quark–gluon evolutions. To this end, we have to include in our discussion not only the QCD-penguin operator Q_6 but also Q_4 defined in (11). Its hadronic matrix element at the factorization scale is given by

$$\langle \pi^+\pi^-|Q_4(0)|K^0\rangle = \langle \pi^0\pi^0|Q_4(0)|K^0\rangle = X_F. \tag{81}$$

Then the 4×4 anomalous dimension matrix in the $Q_{1,2,4,6}$ basis, which through (12) governs the evolution of operators in the quark–gluon (QG) picture, reads [10]:

$$\gamma^{QG} = \frac{\alpha_s N}{2\pi}\begin{pmatrix} 0 & 3/N & 0 & 0 \\ 3/N & 0 & 1/3N & 1/3N \\ 0 & 0 & 0 & 0 \\ 0 & 0 & 0 & -3 \end{pmatrix} = \begin{pmatrix} 0 & 0.286 & 0 & 0 \\ 0.286 & 0 & 0.032 & 0.032 \\ 0 & 0 & 0 & 0 \\ 0 & 0 & 0 & -0.859 \end{pmatrix} \tag{82}$$

in the large-N limit. Recall that $\alpha_s N$ is N-independent to preserve asymptotic freedom in large N QCD. The numerical values above have been obtained for $\alpha_s = 0.6$, namely around the scale 0.8 GeV (see Table 3). This will allow us a comparison of the meson and quark–gluon evolutions.

Using the evolutions (72) and (73) and evaluating the derivatives of $Q_1(M^2)$ and $Q_2(M^2)$ with respect to M^2, we find first

$$M^2\frac{d\,Q_1(M^2)}{dM^2} = -M^2\frac{d\,c_1(M^2)}{dM^2}Q_2(0), \tag{83}$$

$$M^2\frac{d\,Q_2(M^2)}{dM^2} = -M^2\frac{d\,c_1(M^2)}{dM^2}Q_1(0) + M^2\frac{d\,c_2(M^2)}{dM^2}[Q_2(0) - Q_1(0)]. \tag{84}$$

But

$$Q_4(0) = [Q_2(0) - Q_1(0)],$$
$$Q_6(0) = -\frac{r^2(\mu)}{\Lambda_\chi^2}[Q_2(0) - Q_1(0)] \tag{85}$$

in our octet approximation. Thus

$$Q_4(0) + Q_6(0) = \left(1 - \frac{r^2(\mu)}{\Lambda_\chi^2}\right)[Q_2(0) - Q_1(0)]. \tag{86}$$

Therefore, comparing (83) and (84) with (12) for $\mu = M$, we find the non-vanishing elements of the "anomalous dimension matrix" γ^M governing the evolution of operators in the meson (M) picture:

$$\gamma_{12}^M = \gamma_{21}^M = 2M^2\frac{\partial c_1(M^2)}{\partial M^2} > 0, \tag{87}$$

$$\gamma_{24}^M = \gamma_{26}^M = 2M^2\frac{\Lambda_\chi^2}{r^2 - \Lambda_\chi^2}\frac{\partial c_2(M^2)}{\partial M^2} > 0. \tag{88}$$

As $c_{1,2}(M^2) = \mathcal{O}(1/N)$ the signs and the structure of $1/N$ terms in γ^M are precisely the same as in (82), but due to the M^2 dependence of γ_{ij}^M the evolution of operators is faster in the meson evolution when the meson theory includes only the pseudoscalar octet. The diagonal term γ_{66} in (82) is $\mathcal{O}(1)$ and originates in the μ-dependence of quark masses. As discussed at the end of this section, in this case there is a perfect matching between quark–gluon and meson evolutions in the large N limit.

In order to complete the calculation of the anomalous dimension matrix in the meson theory we still need the value of r^2/Λ_χ^2. This value is known in our approach and given in (102). Using this value we find at $M=\mu=0.8$ GeV

$$\gamma_{12}^M=\gamma_{21}^M=0.624,\qquad \gamma_{24}^M=\gamma_{26}^M=0.051,\quad \text{(P)}. \tag{89}$$

We observe that the hierarchy of the elements of the quark–gluon anomalous dimension matrix in (82) is also found in the corresponding matrix in the meson theory. In particular we find

$$\frac{\gamma_{12}^M}{\gamma_{26}^M}=12.2,\qquad \frac{\gamma_{12}^{QG}}{\gamma_{26}^{QG}}=9\qquad \text{(P)}, \tag{90}$$

which is a satisfactory result considering that we have included only pseudoscalar mesons at this level.

We observe that already the inclusion of pseudoscalar mesons allows a reasonable matching between the two anomalous dimensions in question. On the other hand, as emphasized in [11], while the vacuum insertion method gives consistent results for the leading in N contributions, viewed as a meson evolution, it completely misrepresents the next-to-leading effects. Indeed in this case the usual $1/N$ Fierz terms give

$$\langle Q_1(M^2)\rangle_{\rm VIA}=\langle Q_1(0)\rangle+\frac{1}{N}\langle Q_2(0)\rangle, \tag{91}$$

$$\langle Q_2(M^2)\rangle_{\rm VIA}=\langle Q_2(0)\rangle+\frac{1}{N}\langle Q_1(0)\rangle \tag{92}$$

and consequently

$$c_1=-\frac{1}{3},\qquad c_2=0,\qquad \text{(in VIA)}, \tag{93}$$

in total disagreement with the structure of quark–gluon evolution.

In summary, the structure of meson evolution reviewed above leads to a very simple physical picture [11]. The inclusion of the next-to-leading corrections to hadronic matrix elements can be viewed as the evolution of the operators (*meson evolution*) from zero momentum to M. This short but fast evolution is continued above M as a long but slower evolution of Wilson coefficients (*quark–gluon evolution*) by means of the usual QCD renormalization group equations with respect to μ, with the identification (42).

7.3 Inclusion of vector mesons in $c_1(M^2)$ and $c_2(M^2)$

In the same manner, as we did in the case of $\hat{B}_K$, we can easily include vector meson contributions to the coefficients $c_{1,2}(M^2)$ and consequently into current–current contributions to the amplitudes $\mathrm{Re}A_2$ and $\mathrm{Re}A_0$. This is related to the fact that in the chiral limit the meson evolutions of the $\Delta S=2$ and $\Delta I=3/2$ operators are identical. Keeping pseudoscalar masses in the pseudoscalar contributions but calculating the vector contributions in the chiral limit we simply find

$$c_1(M^2)=c_1^P(M^2)-\frac{1}{4f_\pi^2}\left[\frac{f_\pi}{F_\pi}\right]\times\left[\frac{9}{2}\hat{I}_2(m_V^2)-3m_V^2\hat{I}_3(m_V^2)\right], \tag{94}$$

where the first term including only pseudoscalar contributions is given in (74). Yet, in evaluating this term we have to use $f_\pi(M^2)$ in (31) which includes vector meson contributions. The functions $\hat{I}_i$ are given in (45) and (47).

We also find

$$c_2(M^2)=\frac{1}{2}c_1(M^2)+\frac{9}{8}\frac{m_K^2}{(4\pi f_\pi)^2}\left[\frac{f_\pi}{F_\pi}\right]\ln\left(1+\frac{M^2}{\tilde{m}^2}\right) \tag{95}$$

with $c_1(M^2)$ given in (94).

The values for these coefficients with and without the inclusion of vector meson contributions are given in Table 5. Similar to the case of $f_\pi(M^2)$, we observe significant reduction of the scale dependence of $1-c_1(M^2)$ relevant for $\mathrm{Re}A_2$ relative to the pseudoscalar case which will have profound implications for our numerical analysis of $\mathrm{Re}A_2$ in the next section.

With these results at hand, we can now improve the calculation of the anomalous dimension matrix in the meson theory. Setting again $M=\mu=0.8$ GeV we find

$$\gamma_{12}^M=\gamma_{21}^M=0.524,\quad \gamma_{24}^M=\gamma_{26}^M=0.060\quad \text{(P+V)} \tag{96}$$

and

$$\frac{\gamma_{12}^M}{\gamma_{26}^M}=8.7,\qquad \frac{\gamma_{12}^{QG}}{\gamma_{26}^{QG}}=9,\qquad \text{(P+V)}, \tag{97}$$

which is a significant improvement over the result in (89).

This matching of anomalous dimensions is a remarkable feature of our dual approach and might be traced to the existence of AdS/QCD models which do interpolate between the quark and meson pictures—at least for the amplitudes we are considering. They usually have extra states at higher mass scales but the pseudoscalar and vector mesons are usually an essential part of the duality.

What remains to be done is to analyze how these results depend on $M=\mu$. We show this in Table 6. We draw the following conclusions from this table.

- In the full range of M considered γ_{12}^M is by an order of magnitude larger than γ_{26}^M as is the case in the quark–gluon matrix.
- If only pseudoscalar mesons are included the ratio $\gamma_{12}^M/\gamma_{26}^M$ is closest to 9 for $M\approx 0.7$ GeV, while after the inclusion of vector meson contributions this happens slightly above $M\approx 0.8$ GeV. Therefore we conclude

Table 6 Values of γ_{12}^M and γ_{26}^M as functions of M. P and V indicate whether pseudoscalar and vector mesons have been included or left out

M (GeV)	0.6	0.7	0.8	0.9	1.0	Comments
γ_{12}^M	0.437	0.534	0.624	0.706	0.784	(P)
γ_{26}^M	0.072	0.059	0.051	0.046	0.043	(P)
$\gamma_{12}^M/\gamma_{26}^M$	6.0	9.0	12.2	15.3	18.3	(P)
γ_{12}^M	0.356	0.438	0.524	0.615	0.714	(P + V)
γ_{26}^M	0.076	0.066	0.060	0.058	0.057	(P + V)
$\gamma_{12}^M/\gamma_{26}^M$	4.7	6.7	8.7	10.6	12.4	(P + V)

that most reliable results are obtained in our approach for $M = (0.8–0.9)$ GeV.

- Comparing the size of the matrix elements in Table 6 with those in (82) we indeed confirm that the short meson evolution is faster than the long quark–gluon evolution.

7.4 Penguin operators: $B_6^{(1/2)}$ and $B_8^{(3/2)}$

For the matrix elements of QCD-penguin operator Q_6 and the electroweak penguin operator Q_8 we find [10]

$$\langle\pi^+\pi^-|Q_6(0)|K^0\rangle = -\frac{r^2(\mu)}{\Lambda_\chi^2} X_F\, B_6^{(1/2)}$$
$$= -4\sqrt{2}\left[\frac{m_K^2}{m_s(\mu)+m_d(\mu)}\right]^2 \frac{F_\pi}{\kappa}\, B_6^{(1/2)}, \tag{98}$$

with the same result for $K^0 \to \pi^0\pi^0$ matrix element and [87]

$$\langle\pi^+\pi^0|Q_8(0)|K^+\rangle = 3\left[\frac{m_K^2}{m_s(\mu)+m_d(\mu)}\right]^2 F_\pi\, B_8^{(3/2)}, \tag{99}$$

where

$$\kappa = \frac{\Lambda_\chi^2}{m_K^2 - m_\pi^2} = \frac{F_\pi}{F_K - F_\pi} = 4.93. \tag{100}$$

In (98) and (99) we have introduced the parameters $B_6^{(1/2)}$ and $B_8^{(3/2)}$ in order to compare with lattice results. But in the large N limit in which factorization works we simply have as seen from (78), (79) and (85)

$$B_6^{(1/2)} = B_8^{(3/2)} = 1. \tag{101}$$

Finally, for our numerical studies we quote at $\mu = 0.8$ GeV

$$\frac{r^2(\mu)}{\Lambda_\chi^2} = 8.46\left(\frac{160\ \text{MeV}}{m_s(\mu)+m_d(\mu)}\right)^2, \tag{102}$$

where we used the results from FLAG 2013 [88]

$$m_s(2\ \text{GeV}) = (93.8 \pm 2.4)\ \text{MeV},$$
$$m_d(2\ \text{GeV}) = (4.68 \pm 0.16)\ \text{MeV}. \tag{103}$$

There is no contribution of Q_6 to $K^+ \to \pi^+\pi^0$ in the isospin limit, but in the case of ε'/ε isospin breaking corrections leading to a non-vanishing matrix element $\langle Q_6\rangle_2$ have to be taken into account as implemented in [89] where the full 0^{-+} nonet has been consistently included at $\mathcal{O}(p^2)$. The most recent discussion of this issue with the 0^{-+} octet at $\mathcal{O}(p^4)$ can be found in [90].

It should be stressed that generally the parameters $B_6^{(1/2)}$ and $B_8^{(3/2)}$ are very weakly dependent on the scale μ as the dominant μ dependence of the matrix elements of penguin operators comes from the running quark masses. This dependence in the physical amplitudes is canceled by the μ dependence of the corresponding Wilson coefficients, which for large N can be demonstrated analytically. This cancelation results from the fact that the anomalous dimensions of these operators equal twice the anomalous dimension of the mass operator. The effect of mixing with other operators (see $\gamma_{26} \neq 0$) spoils this exact cancelation but the effect is small and is compensated by contributions from current–current operator Q_2. A detailed numerical analysis in [58] confirms this.

The $1/N$ corrections to the result in (101) are not necessary for the analysis of the $\Delta I = 1/2$ rule, as the Wilson coefficients of QCD-penguin Q_6 are $\mathcal{O}(\alpha_s)$ and therefore these contributions are $\mathcal{O}(1/N^2)$. In the case of Q_8 such corrections could possibly play a role in ε'/ε.

There is no reliable result on $B_6^{(1/2)}$ from lattice QCD. On the other hand one can extract the lattice value for $B_8^{(3/2)}$ from $\text{Re}A_2$ in [40]. We find

$$B_8^{(3/2)}(3\ \text{GeV}) = 0.65 \pm 0.05 \qquad \text{(lattice)}. \tag{104}$$

Even if $B_8^{(3/2)}$ is scale independent in the large N limit, it is useful to check its scale dependence in the short-distance regime by means of renormalization group evolution, this time for the matrix element of Q_8, not for its Wilson coefficient. Such an exercise has been performed in [58] with the result that this dependence is at the level of a few percent for 1.0 GeV $\leq \mu \leq$ 3 GeV and even if $B_8^{(3/2)}$ decreases with increasing scale the difference between lattice result and large N result cannot be explained by such effects. On the other hand, the calculation of $1/N$ corrections to (101) in the framework of truncated meson theory of Sect. 3 shows

that while these corrections are small in the case of $B_6^{(1/2)}$, the effect is much larger in the case of $B_8^{(3/2)}$ [31]. Typically $B_8^{(3/2)}$ is found in the ballpark of 0.6 ± 0.1. Consequently also in this case the large N approach seems to give a result similar to the lattice one. Yet, one has to admit that the precision of the calculation in [31] is insufficient for a useful phenomenology of ε'/ε, where there is a strong cancelation between QCD-penguin and electroweak penguin contributions. On the other hand, both lattice calculations and large N approach indicate that $B_8^{(3/2)} < 1$, suppressing electroweak penguin contributions to ε'/ε relative to strict large N limit. This is a hint that ε'/ε in the Standard Model is larger than previously expected. Yet, the future of ε'/ε depends on the result for $B_6^{(1/2)}$ in lattice QCD although it may still take some time before an accurate result for this important quantity is available [43].

8 $\Delta I = 1/2$ rule in the dual QCD approach

8.1 Preliminaries

With all these results at hand, we will now make a closer look at the dynamics of the $\Delta I = 1/2$ rule which follows from our approach. Even without entering the details of the size of the amplitudes involved, we note that the amplitude $A(K^0 \to \pi^0\pi^0)$ enters $\mathrm{Re}A_0$ and $\mathrm{Re}A_2$ in (69) and (70) with the opposite sign. While this feature is at the basis of the difference between A_0 and A_2 and consequently fundamental for the explanation of the $\Delta I = 1/2$ rule, the main dynamics behind the $\Delta I = 1/2$ rule is that $A(K^0 \to \pi^0\pi^0)$ has the same sign as $A(K^0 \to \pi^+\pi^-)$. That this is indeed the case follows both from the explicit evaluation of these amplitudes in our dual representation of QCD and also from our simple picture of the slow quark–gluon evolution from $\mathcal{O}(M_W)$ down to $\mathcal{O}(1\ \mathrm{GeV})$ followed by the fast meson evolution down to $\mu = \mathcal{O}(m_\pi)$. We will now discuss these issues in explicit terms by updating our analysis of the amplitudes $\mathrm{Re}A_0$ and $\mathrm{Re}A_2$ presented first in [11].

8.2 Hadronic matrix elements

The values for hadronic matrix elements of current–current operators in (78) and (79) are simply the initial conditions for the meson evolution, analogous to the initial conditions for Wilson coefficients $z_1(M_W^2)$ and $z_2(M_W^2)$ in the case of quark–gluon evolution that are usually evaluated perturbatively at the high-energy scale. Combining then the initial conditions in (78) and (79) with the meson evolution formulas in (72) and (73) allows us to evaluate the hadronic matrix elements of current–current operators at $\mu = M$ [11]:

$$\langle \pi^+\pi^-|Q_1(M^2)|K^0\rangle = -c_1(M^2)X_F,$$
$$\langle \pi^+\pi^-|Q_2(M^2)|K^0\rangle = \left(1 + c_2(M^2)\right) X_F, \tag{105}$$
$$\langle \pi^0\pi^0|Q_1(M^2)|K^0\rangle = -X_F,$$
$$\langle \pi^0\pi^0|Q_2(M^2)|K^0\rangle = \left(c_1(M^2) + c_2(M^2)\right) X_F, \tag{106}$$
$$\langle \pi^+\pi^0|Q_{1,2}(M^2)|K^+\rangle = \left(1 - c_1(M^2)\right) \frac{X_F}{\sqrt{2}}. \tag{107}$$

where X_F has been defined in (80).

Using (7), (69), (70), the matrix elements (105)–(107) and (98) with $B_6^{(1/2)} = 1$ we find then

$$\mathrm{Re}A_0 = \frac{G_F}{\sqrt{2}} V_{ud} V_{us}^* \left(\frac{1}{3}\right) \times \left[-z_1(1+2c_1) + z_2(2 + c_1 + 3c_2) - 3z_6 \frac{r^2}{\Lambda_\chi^2}\right] X_F \tag{108}$$

$$\mathrm{Re}A_2 = \frac{G_F}{\sqrt{2}} V_{ud} V_{us}^* \left(\frac{2}{3}\right) (1 - c_1)(z_1 + z_2) \frac{X_F}{\sqrt{2}} = 2.54\ (1 - c_1)(z_1 + z_2)\ 10^{-8}\ \mathrm{GeV}, \tag{109}$$

where in order to simplify the notations we did not show the scale dependence of z_i and c_k, explicitly. They all are evaluated at $\mu = M$.

8.3 Diagrammatic understanding of signs

In order to get a better understanding of different signs in (108) and (109) and eventually to compare with the results of the RBC-UKQCD collaboration [37–40], we will use the diagrammatic language developed by us in the context of our first paper on large N approach to weak decays that we applied for the decays $D^0 \to K^+\pi^-$ and $D^0 \to \bar{K}^0\pi^0$ [52][6]. This diagrammatic language inspired by the work of 't Hooft [13,14] and subsequently Witten [15,16] is discussed in detail for the case of non-leptonic K decays in [19–21]. See also [8].

It is clear from these papers, but it should be emphasized again, that the diagrams discussed by us should not be considered as ordinary Feynman diagrams as each of the closed loops stands for sum over all possible planar gluon exchanges.

In Fig. 1 we show four basic current–current diagrams contributing to $K^0 \to \pi^+\pi^-$ and $K^0 \to \pi^0\pi^0$ amplitudes. The four diagrams contributing to $K^+ \to \pi^+\pi^0$ can be obtained from these diagrams by replacing the spectator quark d by the spectator quark u. The wiggly line represents the insertion of the Q_2 operator, while the dashed one the insertion of Q_1 operator. The crosses represent the external mesons. The

[6] See Figs. 10–11 in [52]. Note that the indices of Q_1 and Q_2 are interchanged in that paper.

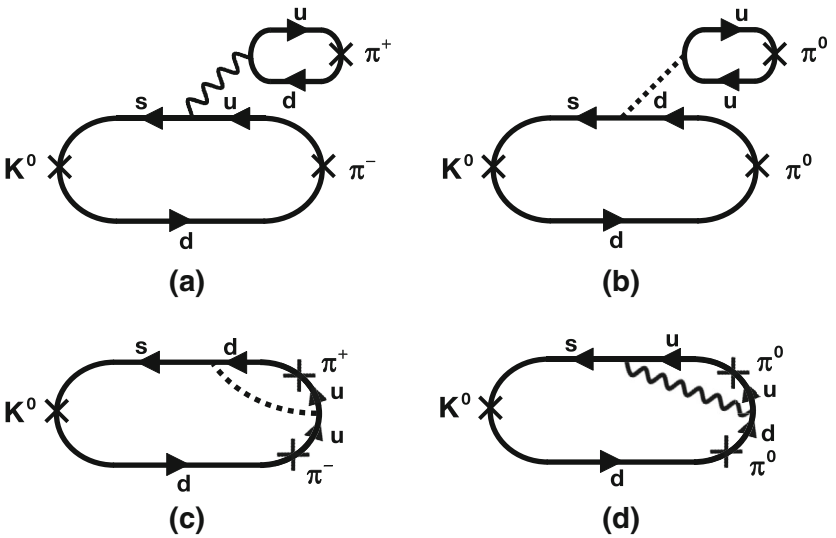

Fig. 1 Current–current topologies in $K \to \pi\pi$

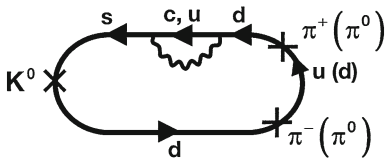

Fig. 2 Penguin topology in $K \to \pi\pi$

Feynman rule for them is the usual color normalization factor $1/\sqrt{N}$ but this universal rule does not interest us here. It is more important that each loop brings a factor N so that the diagrams (c) and (d) are suppressed relative to (a) and (b) by a factor of N. In Fig. 2 we show penguin diagrams that contribute only to $K^0 \to \pi^+\pi^-$ and $K^0 \to \pi^0\pi^0$ amplitudes in the isospin limit.

The results for the matrix elements in (105)–(107) can be reproduced from these diagrams by using the following Feynman-like rules:

Rule 1: Factor X_F for diagrams (a) and (b) in Fig. 1.

Rule 2: Factor $c_1 X_F$ for diagrams (c) and (d) in Fig. 1.

Rule 3: Factor $c_2 X_F$ for penguin diagrams in Fig. 2.

Rule 4: Statistical factor -1 for each quark loop.

Rule 5: Factor -1 when the final neutral pion is created through its $\bar{d}d$ component.

Rule 6: Factor -1 in the penguin diagrams due to the GIM partial cancelation at work ($V_{cd}V_{cs}^* = -V_{ud}V_{us}^*$).

As the factorizable contribution X_F is positive, the dynamics of the $\Delta I = 1/2$ rule is governed by the non-factorizable topologies in (c) and (d) represented by the coefficient $c_1(M^2)$ and it is essential that this coefficient is also positive. In our approach, this positive sign follows in two ways:

- From explicit calculation of loop diagrams in the meson theory.
- From the matching of anomalous dimensions γ^{QG} and γ^{M}.

This understanding of the sign of $c_1(M^2)$ will allow us in Sect. 9 to understand the signs of contractions in the recent results on $\mathrm{Re}A_0$ on $\mathrm{Re}A_2$ from the RBC-UKQCD collaboration [37]. But first we present our own view on these amplitudes.

8.4 The anatomy of the $\Delta I = 1/2$ rule

We are now ready to have a closer look at the basic dynamics behind this rule which in our approach is based on two pillars of QCD: asymptotic freedom at short-distance scales and confinement of quarks in mesons at long-distance scales. The dual representation of QCD as a theory of weakly interacting mesons allows one to unite these two properties in a framework which enables us to see and calculate analytically the observed enhancement of $\mathrm{Re}A_0$ and suppression of $\mathrm{Re}A_2$.

- In the strict large N limit, no evolution takes place:

$$z_1 = 0, \quad z_2 = 1.0, \quad z_6 = 0, \quad c_1 = c_2 = 0. \tag{110}$$

Then only the operator Q_2 contributes and its factorized hadronic matrix elements imply a vanishing $K^0 \to \pi^0\pi^0$ decay amplitude. Consequently

$$R = \frac{\mathrm{Re}A_0}{\mathrm{Re}A_2} = \sqrt{2}, \qquad \text{(in large } N \text{ limit)} \tag{111}$$

in plain disagreement with experiment. The same applies for separate amplitudes as seen in (6).

In this starting point, hadronic matrix elements are evaluated in the free meson theory, which corresponds to the factorization scale $\mu = \mathcal{O}(m_\pi)$, while the Wilson coefficients are calculated in a free (from the point of view of strong interactions) theory of quarks, which corresponds

to scales $\mu = \mathcal{O}(M_W)$ and setting $\alpha_s(M_W) = 0$. In the following steps the gap between these two vastly different energy scales is filled with the QCD dynamics present in quark–gluon and meson evolutions.

- The inclusion of a long but slow logarithmic quark–gluon evolution from $\mu = M_W$ down to $\mu = \mathcal{O}(1\ \text{GeV})$, termed in the past as *octet enhancement* [91,92], generates the operator Q_1 and modifies z_2 so that now

$$z_1 < 0, \quad z_2 > 1.0, \quad z_6 = 0, \quad c_1 = c_2 = 0, \tag{112}$$

where we did not include yet QCD-penguin contribution. Evaluating the Wilson coefficients of Q_1 and Q_2 at a scale $\mathcal{O}(1\ \text{GeV})$ but keeping their hadronic matrix elements at $\mu = 0$, we find an enhancement of R by roughly a factor of two in the NDR-$\overline{\text{MS}}$ scheme, but more like three in the $\overline{\text{MOM}}$ scheme. This difference is then canceled by the scheme dependence of hadronic matrix elements but this fact shows that the size of this enhancement attributed to quark–gluon evolution (Wilson coefficients) and separately to meson evolution (hadronic matrix elements) is both dependent on μ and the renormalization scheme considered. As we use $\overline{\text{MOM}}$ scheme in our paper, we quote using Table 3

$$R_{\text{cc}}(\mu) = \sqrt{2}\left(\frac{z_2(\mu) - z_1(\mu)/2}{z_2(\mu) + z_1(\mu)}\right) \approx 3.1\sqrt{2} \approx 4.4 \quad (\mu = 0.8\ \text{GeV}), \tag{113}$$

where with the index "cc" we indicate that only current–current operator contributions have been taken into account. In the NDR-$\overline{\text{MS}}$ scheme we find $R_{\text{cc}} \approx 3$ instead. For the amplitudes at this stage we find in the $\overline{\text{MOM}}$ scheme at $\mu = 0.8\ \text{GeV}$

$$\text{Re}A_0 = 7.1 \times 10^{-8}\ \text{GeV}, \quad \text{Re}A_2 = 1.6 \times 10^{-8}\ \text{GeV}, \quad (\text{QG evolution}). \tag{114}$$

This means an enhancement of $\text{Re}A_0$ by a factor of 2.0 and suppression of $\text{Re}A_2$ by a factor of 1.6 relative to the large N limit values in (6). While this result is very encouraging, we should note that out of the missing factor of 15.8 for R in the large N limit we have explained only 3.2. Therefore we have to include also QCD dynamics below $\mu = 0.8\ \text{GeV}$.

- In our approach, switching next the short but fast quadratic meson evolution from $\mu = 0$ to $\mu = \mathcal{O}(1\ \text{GeV})$ in order to match the quark evolution provides additional enhancement of $\text{Re}A_0$ and additional suppression of $\text{Re}A_2$ due to positive values of the coefficients c_1 and c_2:

$$R_{\text{cc}} = \sqrt{2}\left\{\frac{z_2(1 + c_1/2 + 3c_2/2) - (z_1/2)(1 + 2c_1)}{(z_2 + z_1)(1 - c_1)}\right\} \approx 12.4, \tag{115}$$

where we quoted the value obtained for $\mu = 0.8\ \text{GeV}$. This is only 40 % below the experimental value in (2) but does not yet include penguin contributions that will enhance R in the direction of experimental value. Yet, already with this dynamics we succeeded to explain the factor 8.7 out of required factor of 15.8, that is, an order of magnitude enhancement of R_{cc} of which 3.1 is attributed to QG evolution and 2.8 to the M evolution.
For the amplitudes, at this stage we find in the $\overline{\text{MOM}}$ scheme at $\mu = 0.8\ \text{GeV}$

$$\text{Re}A_0 = 13.3 \times 10^{-8}\ \text{GeV}, \text{Re}A_2 = 1.07 \times 10^{-8}\ \text{GeV}, \quad (\text{QG} + \text{M evolution}) \tag{116}$$

We would also like to emphasize that for $c_2 = 0$ the amplitude $\text{Re}A_2$ would remain unchanged but $\text{Re}A_0$ would decrease relative to (116)

$$\text{Re}A_0 = 9.1 \times 10^{-8}\ \text{GeV}, R_{\text{cc}} = 8.5, \quad (\text{QG} + \text{M evolution}, \ c_2 = 0). \tag{117}$$

This tells us that the presence of mixing between Q_2 and Q_6 operators represented by c_2 in the meson theory plays a larger role than c_1 in enhancing $\text{Re}A_0$ but has no impact on $\text{Re}A_2$.

- Finally the contribution from the penguin operators, in particular from Q_6, pointed out in [24], has to be taken into account. This operator contributes only to $\text{Re}A_0$ in the isospin limit. Its Wilson coefficient z_6 is negative and GIM suppressed for μ significantly larger than m_c. But as shown in [24] if it is evaluated at μ as low as few hundreds MeV, it then provides the dominant bulk of the enhancement of $\text{Re}A_0$. Even if perturbation theory breaks down at such low scales, it is evident from our approach that at such scales the meson evolution has only very minor contribution to matrix elements of current–current operators. In our case we have for $\mu = \mathcal{O}(1\ \text{GeV})$

$$R_p(\mu) = \frac{3\sqrt{2}}{2}\left(-\frac{r^2(\mu)}{\Lambda_\chi^2}\right)\left(\frac{z_6(\mu)}{z_2(\mu) + z_1(\mu)}\right). \tag{118}$$

At these scales the QCD-penguin contribution to $\text{Re}A_0$ gets smaller than in [24], but, as we will see below, it is still significant.

In summary taking all effects into account we end up with

$$R_{\text{tot}} = R_{\text{cc}} + \frac{R_p}{(1 - c_1)}, \tag{119}$$

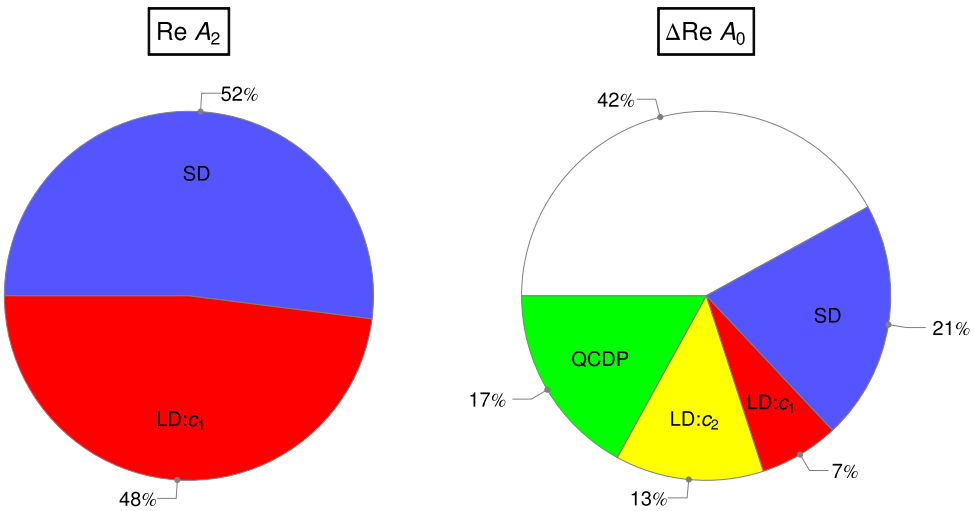

Fig. 3 Budgets for $\mathrm{Re}A_2$ (*left*) and $\Delta\mathrm{Re}A_0$ (*right*) summarizing the size of different suppression mechanisms of $\mathrm{Re}A_2$ and enhancement mechanisms of $\mathrm{Re}A_0$, denoted here by $\Delta\mathrm{Re}A_0$, for the matching scale $\mu = M = 0.8$ GeV. SD stands for quark–gluon evolution and LD for meson evolution. In the case of $\Delta\mathrm{Re}A_0$ we decompose LD into contributions coming from c_1 and c_2. QCDP stands for Q_6 contribution. See text for detailed explanations

where R_p and R_{cc} are given in (118) and (115), respectively. We emphasize again that the relative size of current–current and QCD-penguin contributions to $\mathrm{Re}A_0$ depends on the matching scale μ considered, and the QCD-penguin contribution decreases with increasing μ. While in our case the latter contribution will amount to more than 15 % of $\mathrm{Re}A_0$, in lattice calculations that work at μ = (2–3) GeV, current–current contributions dominate by far and the trace of a significant QCD-penguin contributions found in our case at lower μ should be found in the hadronic matrix element of the current–current operator Q_2. Clearly the final amplitudes cannot depend on the chosen matching scale, but relative contributions are μ-dependent.

With this insight, before presenting graphically the budget of various contributions in Fig. 3, we will present the results for $\mathrm{Re}A_0$ and $\mathrm{Re}A_2$ for other values of M with and without vector meson contributions but always matching in the $\overline{\mathrm{MOM}}$ schemes as well as using the input of 2014.

8.5 Numerical analysis

In Table 1 we give the values of various quantities that we kept fixed in our analysis. In particular the value of m_s relevant for QCD-penguin contribution has been evaluated at $\mu = 0.8$ GeV. The values of $c_{1,2}(M^2)$ including and leaving out vector meson contributions are given in Table 5.

Before presenting our results we would like to address the following problems and state our solutions to them:

- Concerning meson evolution, in the case when only pseudoscalars are included, our results can only be trusted up to the scale $M = 0.6$ GeV. When vector mesons are included this range can be extended to scales M = (0.8–0.9) GeV.
- Concerning quark–gluon evolution one would ideally stop it around the scales explored by lattice calculations, that is, μ = (2–3) GeV. But this is clearly impossible in our approach and we have to evaluate the coefficients at scales μ as low as 1 GeV and even 0.8 GeV. As explained above we have evaluated the Wilson coefficients at NLO in the $\overline{\mathrm{MOM}}$ scheme, which is the scheme to be used to match with the meson evolution. The differences between $\overline{\mathrm{MOM}}$ scheme and NDR-$\overline{\mathrm{MS}}$ as shown in Table 3 are sizable with the short-distance effects being significantly larger in the $\overline{\mathrm{MOM}}$ scheme. Therefore in this scheme, as demonstrated already, the $\Delta I = 1/2$ rule is more visible in the Wilson coefficients than in the NDR-$\overline{\mathrm{MS}}$ scheme used by lattice groups. This difference must then be compensated by the corresponding values of hadronic matrix elements.

When vector meson contributions are taken into account, but higher resonances are not included, it is plausible that the optimal matching scale is $M = \mu = 0.8$. Indeed at this scale the evaluation of both the contributions from the meson and the quark–gluon evolutions can be trusted, even if we cannot claim precision. However, it will be instructive to provide the results also for the full range of 0.6 GeV $\leq \mu = M \leq 1.0$ GeV with and without vector meson contributions in order to see how good the matching is.

In Table 7 we show the results for $\mathrm{Re}A_2$ and $\mathrm{Re}A_0$ including only current–current contributions and calculating Wilson coefficients in the $\overline{\mathrm{MOM}}$ scheme. We indicate by P and V which meson contributions have been included. We observe:

- For scales $M \approx 0.8$ GeV $\mathrm{Re}A_2$ is typically suppressed by a factor of 2.4 relative to the strict large N limit, which is slightly more than required by the data. Moreover, in the absence of vector meson contributions $\mathrm{Re}A_2$

Table 7 The anatomy of the current–current contributions to the $\Delta I = 1/2$ rule as function of the matching scale. P and V indicate that pseudoscalar and vector mesons have been included

$M = \mu$ (GeV)	0.6	0.7	0.8	0.9	1.0	Comments	Data
$10^8 \mathrm{Re}A_2$ (GeV)	1.06	1.04	0.97	0.88	0.77	(P)	1.21
$10^8 \mathrm{Re}A_2$ (GeV)	1.11	1.11	1.07	1.00	0.91	(P + V)	1.21
$10^8 \mathrm{Re}A_0$ (GeV) (cc)	14.2	13.7	13.6	13.6	13.7	(P)	27.0
$10^8 \mathrm{Re}A_0$ (GeV) (cc)	13.9	13.4	13.3	13.4	13.6	(P + V)	27.0
R_{cc}	13.4	13.2	14.0	15.5	17.8	(P)	22.4
R_{cc}	12.5	12.0	12.4	13.4	14.9	(P + V)	22.4

Table 8 The values of $c_1(M^2)$ extracted from the data on $\mathrm{Re}A_2$ for different values of the matching scale in $\overline{\mathrm{MOM}}$ and NDR-$\overline{\mathrm{MS}}$ scheme

M (GeV)	0.6	0.7	0.8	0.9	1.0	Scheme
c_1	0.133	0.201	0.244	0.272	0.295	$\overline{\mathrm{MOM}}$
c_1	0.338	0.355	0.369	0.379	0.389	NDR-$\overline{\mathrm{MS}}$ scheme

drops quickly down with increasing M. The inclusion of vector meson contributions softens significantly this suppression. Even if at $\mu = 0.8$ GeV the amplitude $\mathrm{Re}A_2$ is found by 12 % below the experimental value, this result should be considered as a success of our approach. Indeed $\mathrm{Re}A_2$ is rather close to the data after the vector meson contributions have been included. This allows us to expect that a more complete treatment including heavier resonances could further improve the matching conditions and agreement with experiment.

- The amplitude $\mathrm{Re}A_0$ turns out to be rather insensitive to the inclusion of vector contributions. At $M = 0.8$ GeV roughly 50 % of its experimental value is described by current–current contributions. This could appear disappointing but one should remember that in the case of the $K^0 \to \pi^0\pi^0$ amplitude only the first non-vanishing term in $1/N$ expansion has been included. Still $\mathrm{Re}A_0$ is enhanced by a factor of 3.7 over its leading term which should be regarded as a significant achievement. Moreover, as we will see soon, QCD-penguin contributions help bring $\mathrm{Re}A_0$ closer to the data.

Concerning $\mathrm{Re}A_2$ we may ask what are the values of $c_1(M^2)$ that would reproduce exactly the experimental value of $\mathrm{Re}A_2$. Following (109), such values are given by

$$c_1(M^2) = 1 - \frac{0.476}{(z_1(M) + z_2(M))}. \tag{120}$$

We show the result of this exercise in Table 8. We emphasize the scheme dependence of this result.

In order to complete the analysis we have to include QCD-penguin contributions which further enhance $\mathrm{Re}A_0$. In this context, we would like to recall the analysis in [10] where the effects of an incomplete GIM mechanism above m_c on the mixing between current–current operators and the value of z_6 have been estimated. It has been found that these effects could, at scale $\mu = (0.8\text{–}1.0)$ GeV, enhance $|z_6|$ by a factor of $2 - 3$ relative to the leading order result in which GIM is assumed to be exact for $\mu \geq m_c$. In Table 9 we show our final result at $M = \mu = 0.8$ GeV, including vector meson contributions for different values of the product $|z_6|B_6^{(1/2)}$. Its value 0.04 corresponds to the exact GIM mechanism above m_c and $B_6^{(1/2)} = 1.0$. The remaining values 0.06–0.14 correspond to the effect of the incomplete GIM mechanism above m_c estimated in [10] and/or values $B_6^{(1/2)}$ above unity. However, as seen in Table 9 even for $|z_6|B_6^{(1/2)} = 0.20$ the experimental value of $\mathrm{Re}A_0$ cannot be fully reproduced.

Table 9 $\mathrm{Re}A_2$, $\mathrm{Re}A_0$, and R_{tot} including QCD-penguin contribution for different values of $|z_6|B_6^{(1/2)}$ and the matching scale $M = 0.8$ GeV. Both P and V are included. $\overline{\mathrm{MOM}}$ scheme for z_i has been used

$\lvert z_6\rvert B_6^{(1/2)}$	0.04	0.06	0.08	0.10	0.12	0.14	0.20	Data
$10^8 \mathrm{Re}A_2$ (GeV)	1.07	1.07	1.07	1.07	1.07	1.07	1.07	1.21
$10^8 \mathrm{Re}A_0$ (GeV) (tot)	15.1	16.0	17.0	17.9	18.8	19.7	22.4	27.0
R_{tot}	14.1	15.0	15.8	16.7	17.5	18.4	20.9	22.4

In summary, we observe that our approach provides an order of magnitude enhancement of R relative to the strict large N result $R = \sqrt{2}$. This enhancement follows mainly from the suppression of $\mathrm{Re}A_2$ by a factor of 2.4 and the enhancement of $\mathrm{Re}A_0$ by a factor of 3.7 from current–current contributions. In this manner we improve significantly on the original work on octet enhancement [91,92] where only quark–gluon evolution has been taken into account and the result was scale and renormalization scheme dependent. Including QCD-penguin contributions the latter enhancement increases to 4 in the case of exact GIM above $\mu = m_c$ and could be even as high as 5 if the effects of incomplete GIM are taken into account. In this manner the main bulk (factor 10–12) of the observed enhancement of R relative to $R = \sqrt{2}$ by a factor of 15.8 can be explained.

On the other hand while $\mathrm{Re}A_2$ is found only 12 % below the data, $\mathrm{Re}A_0$ is found to be 40 % smaller than its measured value when strict GIM mechanism is assumed above the charm scale. Our analysis shows therefore that at the scales

we are working QCD-penguin dynamics in the amplitude $\mathrm{Re}A_0$ is relevant. The missing 40 % in $\mathrm{Re}A_0$ can be attributed to the effects of higher resonances in the meson evolution for current–current operators, higher $1/N$ corrections and, as stated above and seen in Table 9, to non-GIM effects above the charm scale and increased value of $B_6^{(1/2)}$. As our calculation of vector meson contributions has been performed in the chiral limit, also here some improvements are possible. A full AdS/QCD description should be able to provide a more complete picture of the long-distance terms and the matching of the amplitudes to the expected short-distance behavior. It would also constrain any purely non-perturbative contribution not directly accessible through current–current operator evolution and matching, such as the one from the $\Delta I = 1/2$ weak mass operator $(mU^\dagger + \text{h.c.})_{ds}$ coupled to either the gluonic term [93] or the quark mass term of the strong trace anomaly [94].

For higher matching scales as μ = (2–3) GeV, used in lattice calculations, the role of QCD-penguins in $\mathrm{Re}A_0$ will be much smaller. The incomplete GIM effects above m_c discussed here should then be found dominantly in the enhanced hadronic matrix elements of current–current operators, in particular Q_2. The comparison with latest lattice analyses is given in the next section.

Finally, in Fig. 3 we show budgets for $\mathrm{Re}A_2$ (left) and $\mathrm{Re}A_0$ (right) that summarize the size of different suppression mechanisms of $\mathrm{Re}A_2$ and enhancement mechanisms of $\mathrm{Re}A_0$[7]. SD stands for quark–gluon evolution and LD for meson evolution. In the case of $\mathrm{Re}A_0$ we decompose LD into contributions coming from c_1 and c_2. QCDP stands for Q_6 contribution. We set the matching scale at $\mu = 0.8$ GeV.

In the case of $\mathrm{Re}A_2$ the division into SD and LD contributions is straightforward as seen in (109). We find then that 52 % of suppression of $\mathrm{Re}A_2$ comes from SD (*violet*) and 48 % from LD (*red*). The color coding expresses the ultraviolet and infrared character of the two contributions, respectively.

The case of $\mathrm{Re}A_0$ is more complicated in view of the fact that penguin contributions are present, the LD contributions involve the coefficients c_1 and c_2 and finally, as we have seen, we are not able to explain fully the missing $\Delta\mathrm{Re}A_0 = 23.4 \times 10^{-8}$ GeV relative to the large N limit. We will normalize different contributions in the budget to this additive contribution required by the data. Following [10] we will assume that due to incomplete GIM mechanism above m_c QCD-penguin contributions are enhanced at $\mu = 0.8$ GeV by a factor of two so that $|z_6|B_6^{(1/2)} = 0.08$. Using the results in Table 9 we find then that 42 % of the missing shift in $\mathrm{Re}A_0$ remains presently unexplained and we present it in *white*. In this normalization QCD-penguin contribution amounts to 17 % and corresponds to the *green* area with the color chosen to express the character of this particular contribution.

The division between SD and LD current–current contributions to $\Delta\mathrm{Re}A_0$ is complicated by the fact, as seen in (108), that, in contrast to $\mathrm{Re}A_2$, the coefficients of z_1 and z_2 involve different LD factors. Therefore just switching off the LD part or the SD part can only teach us about the relative importance of these two contributions but their sum will miss by a factor of 1.4 the total contribution from octet enhancement that one obtains when these two contributions are simultaneously at work. Correcting for this factor we finally find that the 41 % contribution from octet enhancement of $\Delta\mathrm{Re}A_0$ is, like for $\mathrm{Re}A_2$, almost equally distributed between these two contributions: SD (21 %) and LD (20 %). In order to stress the importance of the mixing of Q_2 and Q_6 operators we divide the LD contribution into two parts so that the effect of c_2 in enhancing $\mathrm{Re}A_0$ is roughly twice as large as the one of c_1. The part of LD related to c_1 is again in *red* but c_2 area representing the mixing of Q_2 and Q_6 or equivalently mixing of *red* and *green* is consequently *yellow*.

Finally, we would like to refer to the analysis in [30] which was done in the spirit of our approach except that for the low-energy meson contributions an extended Nambu–Jona-Lasinio model has been used resulting in differences in the matching between long-distance and short-distance contributions. Also these authors find sizable enhancement of $\mathrm{Re}A_0$ and suppression of $\mathrm{Re}A_2$ but various uncertainties in their model allow them only to quote the range $15 \le R \le 40$. The large value of R originates in a small value of $\mathrm{Re}A_2$ which is more strongly suppressed than required and is typically by 30 % below its experimental value.

9 Comparison with lattice results

We will now compare our results with the results on $\mathrm{Re}A_0$ and $\mathrm{Re}A_2$ from the RBC-UKQCD collaboration [37–40]. As the normalization of $\mathrm{Re}A_0$ and $\mathrm{Re}A_2$ in the latter papers differs from ours, we first have to define

$$\mathrm{Re}A_0 = \sqrt{\frac{2}{3}}(\mathrm{Re}A_0)_L, \qquad \mathrm{Re}A_2 = \sqrt{\frac{2}{3}}(\mathrm{Re}A_2)_L, \tag{121}$$

where subscript L refers to the amplitudes in [37]. The latter are given in terms of contractions ① and ② in Fig. 1 of that paper that correspond to the diagrams (a) and (b) in our Fig. 1, respectively. One has to be careful in this comparison, as in [37] the Fierz transformed form of Q_1 relative to the one in (9) is used. Basically, Q_2 contributes to $K^0 \to \pi^+\pi^-$ and $K^0 \to \pi^0\pi^0$ through contractions ① and ②, respectively, while in the case of Q_1 the role of contractions is interchanged. With this information, the diagrams (c) and (d) in Fig. 1 are automatically included in the results for the amplitudes which read [37]:

[7] We thank Jennifer Girrbach for providing these plots.

Table 10 The two contractions in the NDR-$\overline{\text{MS}}$ scheme for $\mu = 2.15$ GeV and resulting $\text{Re}A_0$ and R for different values of K defined in (126) assuming $\text{Re}A_2$ to agree with data

K	0.50	0.60	0.70	0.80	0.85	0.90
① (GeV^3)	0.0237	0.0296	0.0395	0.0593	0.0791	0.119
② (GeV^3)	−0.0119	−0.0178	−0.0277	−0.0474	−0.0673	−0.107
$10^8\text{Re}A_0$ (GeV)	6.9	9.0	12.6	19.8	27.0	41.3
R	5.7	7.5	10.4	16.4	22.3	34.2

$$(\text{Re}A_0)_L = \frac{G_F}{\sqrt{2}} V_{ud} V_{us}^* \left(\frac{1}{\sqrt{3}}\right) \left[z_1\,(2\,② - ①) + z_2\,(2\,① - ②)\right], \tag{122}$$

$$(\text{Re}A_2)_L = \frac{G_F}{\sqrt{2}} V_{ud} V_{us}^* \sqrt{\frac{2}{3}} (z_1 + z_2)\,(① + ②)\,. \tag{123}$$

Before comparing with our results let us find what values of ① and ② at $\mu = 2.15$ GeV, used in [37], would simultaneously reproduce the data for both amplitudes. With the NDR-$\overline{\text{MS}}$ values $z_1 = -0.287$ and $z_2 = 1.133$ at $\mu = 2.15$ GeV, we find

$$① = 0.0791\ \text{GeV}^3, \quad ② = -0.0673\ \text{GeV}^3, \quad ② = -0.85\,①. \tag{124}$$

It should be emphasized that these results apply to the NDR-$\overline{\text{MS}}$ scheme and, as the contractions represent the matrix elements, they must be both scheme and scale dependent.

Now in [37] $② \approx -0.7\ ①$ is found. However, it should be stressed that this numerical result is not in the NDR-$\overline{\text{MS}}$ scheme but in the lattice scheme used there.[8] The relative sign of these two contractions found in [37] is an important result and agrees with the sign we would obtain using the same language, as discussed in more detail below.

We note also that in our normalization the lattice result for $\text{Re}A_2$ in [40] reads

$$\text{Re}A_2 = (1.13 \pm 0.21) \times 10^{-8}\ \text{GeV}. \tag{125}$$

The error is dominated by systematics. This result is in agreement with the data and, within uncertainties, with our results for $\text{Re}A_2$ in Tables 7 and 9. In fact, though obtained using a different approach, we find it remarkable that the central value in (125) differs from our central value in (116) by only 6 %. This is still another support for the dual picture of QCD.

Not having the Wilson coefficients z_1 and z_2 in the lattice scheme, but expecting that in the future all lattice results will be quoted in the NDR-$\overline{\text{MS}}$ scheme used by phenomenologists, we may nevertheless investigate how the result for $\text{Re}A_0$ depends on the ratio of these two contractions in the latter scheme assuming the data for $\text{Re}A_2$. Defining then the K factor by

$$② = -K\ ① \tag{126}$$

we show in Table 10 the results for the two contractions, $\text{Re}A_0$ and R for different values of K. As we use $z_{1,2}$ in the NDR-$\overline{\text{MS}}$ scheme for $\mu = 2.15$ GeV, these results apply only to this scheme and this scale.

We observe that the final results for the quantities in Table 10 strongly depend on the value of K and for $K \approx 0.7$, the ratio R is in the ballpark of the ratio found in [37], even if a different scheme is used there. Yet, in view of the comments made above and the fact that the lattice result for $\text{Re}A_0$ corresponds to non-physical kinematics this comparison is only on a qualitative level. Still the message is clear. If the ratio K in the NDR-$\overline{\text{MS}}$ scheme will be found significantly smaller than $K = 0.85$ and agreement with the data on $\text{Re}A_2$ will be imposed, a satisfactory description of the data on $\text{Re}A_0$, even at scales μ = 2–3 GeV, will not be possible with ① and ② only. The rescue could come then from other contractions that involve QCD-penguin contributions. These contributions are presently estimated in [37] to be very small. But the situation may change when the calculations are performed at physical kinematics.

Comparing the expressions (122) and (123) with our results in (108) and (109) and taking into account different normalization we can express the contractions ① and ② in terms of X_F and c_1. To this end we have to set $c_2 = 0$ and drop penguin contributions. We find then

$$① = \frac{X_F}{\sqrt{2}}, \qquad ② = -c_1 \frac{X_F}{\sqrt{2}}, \qquad K = c_1. \tag{127}$$

It should be remembered that contractions and also $K = c_1$ are scheme and scale dependent and the ones given here are in the $\overline{\text{MOM}}$ scheme. However, already this result offers the explanation of the *positive* sign of ① and of *negative* sign of ② found in [37]. In particular, the latter sign follows in our approach from the proper matching of the anomalous dimension matrices in the meson and quark–gluon pictures of QCD.[9] Therefore the result obtained in [37] is an important support for our dual QCD approach to weak decays, in particular as the lattice calculations will eventually provide much more precise results than can be obtained in our analytic approach. Even if with $X_F = 0.0298\ \text{GeV}^3$ the values of the contractions in (127) appear at first sight to be much

[8] Chris Sachrajda, private communication.

[9] As a side remark let us note that within VIA $K = c_1 = -1/3$ which is at variance not only with our results but also with the findings in [37].

smaller than the ones collected in Table 10, it can be demonstrated that they are fully compatible with the dynamics at scales $\mathcal{O}(2\ \text{GeV})$.

Indeed, the authors of [37] work at $\mu = 2.15$ GeV and we at $M \approx 0.8$ GeV. Therefore our K factor must be different from the one in lattice calculations. It must be smaller and, as seen in Table 5, this is indeed the case. Therefore the numerical comparison of the results of [37] with ours must also involve the Wilson coefficients z_i. The fact that our approach and lattice approach predict similar values for $\text{Re}A_2$ implies the compatibility of both approaches as far as $\Delta I = 3/2$ transitions are concerned.

The comparison of both approaches in the case of $\text{Re}A_0$ is more difficult because in our approach the QCD-penguin contributions cannot be neglected. Moreover, in our approach the mixing of Q_2 operator with Q_6 operator represented by c_2 constitutes a significant part of the enhancement of $\text{Re}A_0$ in the current–current sector. We have emphasized it in previous sections and in Fig. 3. On the basis of the formulas in (105) and (106) we expect that the latter effects are present in the hadronic matrix elements of the operator Q_2 evaluated at the lattice scales.

In this context it is interesting to note that in the strict large N limit

$$① = 0.0210\ \ \text{GeV}^3, \qquad ② = 0, \qquad (\mu \approx 0) \tag{128}$$

which drastically differs from the values of contractions in Table 10 for $K \geq 0.6$ that correspond to $\mu = 2.15$ GeV. Yet the fast meson evolution and the presence of significant QCD penguin contributions, both through their diagonal evolution and mixing with Q_2 operator, allows us, as seen in Tables 9 and 10, to obtain values of $\text{Re}A_0$ that with the contractions considered in [37] can only be obtained for K as large as $K \approx 0.75$ within the NDR-$\overline{\text{MS}}$ scheme.

This discussion shows that, at least at a semi-quantitative level, the recent lattice results can be interpreted within the dual representation of QCD as a theory of weakly interacting mesons for large N. A more detailed comparison will only possible when lattice results for $\text{Re}A_0$ with physical kinematics will be available.

10 $K_L - K_S$ mass difference

10.1 Preliminaries

We begin our discussion by summarizing the status of short-distance contributions to ΔM_K within the SM. For that purpose we decompose it as follows:

$$\Delta M_K = (\Delta M_K)_{\text{cc}} + (\Delta M_K)_{\text{ct}} + (\Delta M_K)_{\text{tt}} + (\Delta M_K)_{\text{LD}}, \tag{129}$$

with the first three short-distance contributions obtained from usual box diagrams and the last term standing for long-distance contributions. The second and third term contributing at most 1 % to ΔM_K [95,96] will be neglected in what follows. For the dominant contribution we have

$$(\Delta M_K)_{\text{cc}} = \frac{G_F^2}{3\pi^2}\left(V_{ud}V_{us}^*\right)^2 F_K^2 \hat{B}_K m_K \eta_{\text{cc}} m_{\text{c}}^2(m_{\text{c}}). \tag{130}$$

The QCD factor η_{cc} including NLO [97] and NNLO [95] QCD corrections is unfortunately subject to very large uncertainties:

$$\eta_{\text{cc}} = 1.87(76), \tag{131}$$

so that [95]

$$\begin{aligned}(\Delta M_K)_{\text{cc}} &= (3.1 \pm 1.2)10^{-15}\ \text{GeV} \\ &= (0.89 \pm 0.34)(\Delta M_K)_{\text{exp}}\end{aligned} \tag{132}$$

with the experimental value given in (3). We conclude therefore that extracting $(\Delta M_K)_{\text{LD}}$ from the data on the basis of this calculation is impossible as this would imply the range of values between 45 to -21 % of the measured value. As we will demonstrate below, from our approach $(\Delta M_K)_{\text{LD}}$ is known much better and this invited the authors of [96] to use this result for the extraction of η_{cc} from $(\Delta M_K)_{\text{exp}}$. In this manner the uncertainty in the evaluation of ε_K could be reduced.

10.2 $(\Delta M_K)_{\text{LD}}$ in the strict large N limit

We have seen that the large N value for $\hat{B}_K$ is supported by the latest lattice results. So, we feel rather confident about calculating the $K_L - K_S$ mass difference within the same approximation [21,26].

In order to get some feeling for the size of effects, we calculate first $(\Delta M_K)_{\text{cc}}$ in the strict large N limit. In this case $\hat{B}_K = 3/4$ but in addition $\eta_{\text{cc}} = 1$ in (130). Yet for the very low values of scales used for the evaluation on $\hat{B}_K$ we cannot use $m_{\text{c}}(m_{\text{c}})$ but rather its constituent mass $m_{\text{c}} = 1.5 \pm 0.1$ GeV. This rough estimate results in (66 ± 9) % of the measured value attributed to short-distance part and $+(34 \pm 9)$ % to the LD contribution. The important message from this simple exercise is the positivity of $(\Delta M_K)_{\text{LD}}$. Yet, we would like to provide a better estimate.

Applying this strategy but not using the constituent charm quark mass, it is quite convenient to parametrize the full ΔM_K as follows ($B_K = 3/4$):

$$\begin{aligned}\Delta M_K &= \frac{G_F^2}{4\pi^2}\left(V_{ud}V_{us}^*\right)^2 F_K^2 m_K M_\Delta^2 \\ &= (10^{-15}\ \text{GeV}^{-1})M_\Delta^2.\end{aligned} \tag{133}$$

From the experimental value (3) of this mass splitting, we easily extract

$$M_\Delta^{\rm exp} = 1.87\ {\rm GeV}. \tag{134}$$

In the effective Fermi theory, such a scale has been associated with the mass of some new degree of freedom to appear in the UV completion. First misidentified as the mass of a hypothetical W weak boson, this $\Delta S = 2$ scale has then been eventually linked (with the help of the GIM mechanism) to the mass of a yet-to-be-discovered charm quark [98]. Working again in the $m_\pi^2 = 0$ limit, let us estimate M_Δ in the large N limit.

A straightforward calculation of the standard box-diagram involving only virtual charm or (and) up quarks gives then

$$M_\Delta^2({\rm SD}) = m_{\rm c}^2 - M^2 + m_K^2 \ln\left(m_{\rm c}^2/M^2\right) - (5/6)m_K^2 + \mathcal{O}\left(m_K^4/M^2\right), \tag{135}$$

if M is the IR cutoff for the high W-momenta:

$$M^2 < q_W^2 < m_{\rm c}^2. \tag{136}$$

In (135), the relative sign between the first two quadratic terms results from the GIM mechanism at work ($m_u = 0$) while the third logarithmic one arises when keeping the external momentum for the strange quarks ($m_d = 0$).

At long distance, the K and π one-loops generated by $Q_2 \otimes Q_2$ give

$$M_\Delta^2({\rm LD}) = (7/4)M^2 - (3/4)m_K^2 \ln(M^2/m_K^2) + (11/24)m_K^2 + \mathcal{O}(m_K^4/M^2), \tag{137}$$

if M is the UV cutoff for the low W-momenta:

$$0 < q_W^2 < M^2. \tag{138}$$

With this unambiguous identification of the momentum across the SD–LD frontier, we can consistently impose the M-independent condition

$$\partial/\partial M^2 \left[M_\Delta^2({\rm SD}) + M_\Delta^2({\rm LD})\right] = 0 \tag{139}$$

to get an optimal matching scale remarkably close to the light vector meson mass, namely

$$M = \sqrt{\frac{7}{3}} m_K \approx m_V \approx 0.8\ {\rm GeV}. \tag{140}$$

If we vary the cutoff around this natural matching scale (say, $0.5\ {\rm GeV} < M < 1.0\ {\rm GeV}$), the LD contribution relative to the measured ΔM_K mass difference turns out to be (30 ± 15) % in a remarkable agreement with our previous estimate. But within our dual picture of QCD we always have to combine the LD contribution with its complementary, namely the SD one, to get any observable. Doing so with (135) and (137), we now observe a remarkable stability with respect to variations of M in the same energy range:

$$\Delta M_K({\rm SD} + {\rm LD}) = (0.80 \pm 0.10)(\Delta M_K)_{\rm exp}. \tag{141}$$

In fact, the main uncertainty in this large N estimate of the $K_L - K_S$ mass difference arises from the charm quark (constituent) mass taken here to be $m_{\rm c} = (1.5 \pm 0.1)$ GeV.

10.3 Non-leading corrections

In the $1/N$ expansion, leading and subleading contributions to ΔM_K correspond to the same topologies as for the B_K, once the fictitious color-singlet boson is replaced by two physical W's. Consequently, one might expect the $1/N$ corrections to the $K_L - K_S$ mass difference to be negative and thereby modify our previous estimate. As we will show now this is indeed the case for the LD (π, η, and η') pole contributions generated this time by $Q_1 \otimes Q_1$. However, we already know from B_K how a partial $1/N$ estimate can misrepresent the physical world.

Our simple analytical approach can be extended to the full nonet of pseudoscalars (η_0 included) to disentangle the QCD-penguin operator Q_6 from $Q_2 - Q_1$:

$$Q_6(0) = -\left(r^2/\Lambda_\chi^2\right)(Q_2 - Q_1 + Q_3)(0) \tag{142}$$

with the new current–current operator

$$Q_3 = 4(\overline{s_L}\gamma^\mu d_L)(\overline{q_L}\gamma_\mu q_L) \tag{143}$$

proportional to $\partial_\mu \eta_0$. As a result, it can easily be applied to other observables somehow related to the empirical $\Delta I = 1/2$ rule, such as radiative K-decay rates [99] or the $\mathcal{O}(G_F^2 \varepsilon')$ weakly induced strong θ parameter [100]. In the same manner the $1/N$-suppressed (π, η, η') pole contribution to the ΔM_K are found to be [99]

$$\Delta M_K({\rm pole}) \approx -0.3(\Delta M_K)_{\rm exp}, \tag{144}$$

canceling significantly the leading order estimate. Our final estimate of LD contributions to ΔM_K within our approach including estimates of leading and next to leading corrections gives then

$$(\Delta M_K)_{\rm LD} \approx (0.2 \pm 0.1)(\Delta M_K)_{\rm exp}. \tag{145}$$

This result is consistent with the analysis of $(\Delta M_K)_{\rm LD}$ in the context of the calculation of long-distance effects in ε_K [101]. Using it in (129) and (130) and assuming no new physics contributions to ΔM_K, one extracts $\eta_{\rm cc}$ from the data to be [96]

$$\eta_{\rm cc} = 1.7 \pm 0.2 \tag{146}$$

with an error almost four times smaller than the error in the direct calculation in (131). It should be emphasized that this

value should not be confused with $\eta_{cc} = 1$ used in our exercise before as in this extraction $m_c(m_c) = 1.28$ GeV has been used in order to compare with the result in (131). If $m_c = 1.5$ GeV was used instead, we would find $\eta_{cc} = 1.23 \pm 0.15$, fully compatible with $\eta_{cc} = 1$. We note that for the computation of charm contribution to ε_K only the product $\eta_{cc} m_c^2$ enters and if η_{cc} is extracted from experimental value of ΔM_K it is immaterial which of these two values of m_c are used.

Needless to say, we are aware of the fact that our estimate in (145) requires more detailed investigations and in particular future confirmation from lattice simulations. Presently, no reliable result on $(\Delta M_K)_{LD}$ from lattice simulations is available but important progress toward its evaluation has been made in [57]. This first result seems to indicate that $(\Delta M_K)_{LD}$ could be larger than expected by us. We are therefore looking forward to more precise evaluation of this important quantity from the lattice in order to see whether also in this case large N approach passed another test or not.

11 Conclusions

Motivated by the recent advances in the computation of non-perturbative parameters in the Kaon system by several lattice collaborations [41–43], in particular the RBC-UKQCD collaboration, we have reviewed our results obtained in the 1980s within the dual representation of QCD as a theory of weakly interacting mesons for large N. This includes in particular:

- The parameter $\hat{B}_K$,
- The isospin amplitudes $\mathrm{Re}A_0$ and $\mathrm{Re}A_2$,
- $K_L - K_S$ mass difference.

It is remarkable that the recent lattice QCD results using dynamical fermions confirm our finding of 1980s that $\hat{B}_K$ is very close to its large N value. Relative to our first paper on $\hat{B}_K$ [12], where only pseudoscalar meson contributions have been taken into account, the inclusion of vector meson contributions, already advocated by one of us in [21,48], decreased significantly the left-over scale dependence of $\hat{B}_K$ bringing it very close the its large N value of 3/4. The numerical confirmation of this result by a number of lattice groups gives support for our work of 1980s. The smallness of $1/N$ corrections to the large N value $\hat{B}_K = 3/4$ results, within our approach, from an approximate cancelation between the pseudoscalar and vector meson one-loop contributions. This is clearly demonstrated in Table 4.

Concerning $\Delta I = 1/2$ rule our physical explanation, stated already in the abstract and discussed in detail in Sect. 8, is based on the evolution from high-energy scales down to very low-energy scales at which factorization of the hadronic matrix elements into products of current matrix elements in the case of current–current operators and quark densities in the case of QCD-penguin operators is recovered. As the long but slow quark–gluon evolution and short but fast meson evolution involve different degrees of freedom, the matching around the $\mathcal{O}(1\ \mathrm{GeV})$ scale is more challenging than in lattice QCD which works with quarks and gluons only. Yet, as we have shown, when vector meson contributions are included and the Wilson coefficients are calculated in the $\overline{\mathrm{MOM}}$ scheme the matching is very good in the case of $\mathrm{Re}A_0$ but also satisfactory for $\mathrm{Re}A_2$ which is found close to its experimental value and also to its lattice value. We expect that the inclusion of heavier resonances and going beyond the chiral limit estimate of vector meson contributions will further bring the theory closer to the data.

As seen in Table 7, the current–current operators alone can at scales considered by us explain roughly 60 % of the $\Delta I = 1/2$ rule. As pointed out by us in [11], this should be considered as the dominant mechanism of the $\Delta I = 1/2$ rule as it suppresses $\mathrm{Re}A_2$ amplitude and enhances $\mathrm{Re}A_0$. It should be emphasized that the quark–gluon evolution with the present value of α_s is insufficient to suppress $\mathrm{Re}A_2$ in order to reproduce the data. Additional suppression is necessary from hadronic matrix elements. In our approach this is achieved through fast meson evolution, which while suppressing $\mathrm{Re}A_2$ enhances further $\mathrm{Re}A_0$. The recent findings by the RBC-UKQCD lattice collaboration confirm this picture in a spectacular manner in the case of $\mathrm{Re}A_2$, but also the enhancement of $\mathrm{Re}A_0$ in lattice simulations is very interesting. While the latter approach obtains presently $R \approx 11$, the results for $\mathrm{Re}A_0$ are still obtained using non-physical kinematics and improving on this in the future should enhance R toward its experimental value.

Yet, at the scales we are working, QCD-penguins provide a significant contribution to $\mathrm{Re}A_0$, in particular as the value of the strange quark mass decreased relative to our analysis in 1986. We find then $R \approx 16.0 \pm 1.5$ that depends on the size of incomplete GIM mechanism that deserves further study in the $\overline{\mathrm{MOM}}$ scheme together with $1/N$ corrections to the hadronic matrix elements of Q_6. These effects and inclusion of higher mass resonances could provide the explanation of the missing 30 % in $\mathrm{Re}A_0$. The present budgets of different mechanisms suppressing $\mathrm{Re}A_2$ and enhancing $\mathrm{Re}A_0$ in our approach are summarized in Fig. 3.

In the case of lattice calculations normalized around 2 GeV, explicit QCD-penguin contributions to $\mathrm{Re}A_0$ are much smaller as the GIM suppression is still rather effective at these scales. The significant contribution of QCD-penguins should then be found in the enhanced matrix elements of current–current operators, in particular Q_2 operator. In our approach this corresponds to the increased value of the coefficient c_2, which, as seen in Table 5, increases with increased

value of M. This increase, as seen in (108), enhances $\mathrm{Re}A_0$ in addition to the enhancement through c_1.

From the point of view of our approach the RBC-UKQCD lattice collaboration clearly identified the effects in both amplitudes coming from the enhanced value of c_1. The next step would be to separate the enhancement of $\mathrm{Re}A_0$ through c_1 from the one through c_2. This would be signaled by an enhanced matrix elements of the Q_2 operator in $K^0 \to \pi^+\pi^-$ and $K^0 \to \pi^0\pi^0$ decays. It should also be investigated whether the role of QCD-penguin operator Q_6 at these higher scales is indeed as small as presently implied by lattice results. It would also be interesting to perform lattice calculations of hadronic matrix elements at several values of μ including those considered in our paper in order to verify meson evolution of hadronic matrix elements more precisely than can be done in our approach.

While our analytic approach allowed us to identify the dynamics behind the observed $\Delta I = 1/2$ rule, the precision calculations of $\mathrm{Re}A_0$ and $\mathrm{Re}A_2$ can only be obtained from lattice QCD although it will take some time before uncertainties in these amplitudes will be reduced down to 10 % level. Whether the lattice approach will be able, on its own, to provide the physical explanation of the dynamics behind the $\Delta I = 1/2$ rule remains to be seen. It would also be important to make further efforts in the context of realistic AdS/QCD descriptions of the $1/N$ expansion as this should allow more a precise interpolation of the meson amplitudes to scales explored by the lattice community. In this manner, the comparison of the $1/N$ expansion with the unquenched lattice results could be made more explicit. It would also allow a closer look at the upper bound on $\hat{B}_K$ at these higher-energy scales.

In summary, it is quite encouraging that our simple analytic framework improved by the inclusion of vector mesons and proper matching to short-distance Wilson coefficients yields consistent results in good agreement with the data. Simultaneously, it provides a simple picture of the dynamics behind the $\Delta I = 1/2$ rule which as the basis has the main property of QCD: asymptotic freedom and the related evolutions of weak matrix elements which at long-distance scales can be performed in the dual representation of QCD as a theory of weakly interacting mesons for large N.

Acknowledgments AJB would like to thank Gino Isidori and Heiri Leutwyler for very encouraging comments on the first version of the paper and Jure Drobnak and Robert Ziegler for checking numerically the values of the Wilson coefficients z_i. We would like to thank Jennifer Girrbach, Chris Sachrajda and Amarjit Soni for discussions and Nuria Carrasco, Luca Silvestrini and Vittorio Lubicz for E-mail exchanges. This research was financially supported by the ERC Advanced Grant project "FLAVOUR" (267104) and the Belgian IAP Program BELSPO P7/37. It was also partially supported by the DFG cluster of excellence "Origin and Structure of the Universe". Fermilab is operated by Fermi Research Alliance, LLC under Contract No. DE-AC02- 07CH11359 with the United States Department of Energy.

References

1. V. Cirigliano, G. Ecker, H. Neufeld, A. Pich, J. Portoles, Kaon decays in the standard model. Rev. Mod. Phys. **84**, 399 (2012). arXiv:1107.6001
2. Particle Data Group Collaboration, J. Beringer et al., Review of particle physics (RPP). Phys. Rev. D **86**, 010001 (2012)
3. M. Gell-Mann, A. Pais, Behavior of neutral particles under charge conjugation. Phys. Rev. **97**, 1387–1389 (1955)
4. M. Gell-Mann, A. Rosenfeld, Hyperons and heavy mesons (systematics and decay). Annu. Rev. Nucl. Part. Sci. **7**, 407–478 (1957)
5. NA48 Collaboration Collaboration, J. Batley et al., A precision measurement of direct CP violation in the decay of neutral kaons into two pions. Phys. Lett. B **544**, 97–112 (2002). [hep-ex/0208009]
6. KTeV Collaboration Collaboration, A. Alavi-Harati et al., Measurements of direct CP violation, CPT symmetry, and other parameters in the neutral kaon system. Phys. Rev. D **67**, 012005 (2003). [hep-ex/0208007]
7. KTeV Collaboration Collaboration, E. Worcester, The Final Measurement of ε'/ε from KTeV. arXiv:0909.2555
8. A.J. Buras, J.-M. Gérard, $1/N$ Expansion for Kaons. Nucl. Phys. B **264**, 371 (1986)
9. W.A. Bardeen, A.J. Buras, J.-M. Gérard, The $\Delta I = 1/2$ Rule in the Large N Limit. Phys. Lett. B **180**, 133 (1986)
10. W.A. Bardeen, A.J. Buras, J.-M. Gérard, The $K \to \pi\pi$ Decays in the Large N Limit: Quark Evolution. Nucl. Phys. B **293**, 787 (1987)
11. W.A. Bardeen, A.J. Buras, J.-M. Gérard, A Consistent Analysis of the $\Delta I = 1/2$ Rule for K Decays. Phys. Lett. B **192**, 138 (1987)
12. W.A. Bardeen, A.J. Buras, J.-M. Gérard, The B Parameter Beyond the Leading Order of 1/N Expansion. Phys. Lett. B **211**, 343 (1988)
13. G. 't Hooft, A planar diagram theory for strong interactions. Nucl. Phys. B **72**, 461 (1974)
14. G. 't Hooft, A two-dimensional model for mesons. Nucl. Phys. B **75**, 461 (1974)
15. E. Witten, Baryons in the 1/n expansion. Nucl. Phys. B **160**, 57 (1979)
16. S. Treiman, E. Witten, R. Jackiw, B. Zumino, Current algebra and anomalies
17. A.J. Buras, Strangeness and the Large N Expansion. Nucl. Phys. A **479**, 399C–421C (1988)
18. W.A. Bardeen, Weak Decay Amplitudes in Large N QCD. Nucl. Phys. Proc. Suppl. **7A**, 149 (1989)
19. A.J. Buras, The $1/N$ Approach to Nonleptonic Weak Interactions. Adv. Ser. Direct. High Energy Phys. **3**, 575–645 (1989)
20. A.J. Buras, Phenomenological Applications of the $1/N$ Expansion. Nucl. Phys. Proc. Suppl. **10A**, 199–267 (1989)
21. J.-M. Gérard, Electroweak interactions of hadrons. Acta Phys. Polon. B **21**, 257–305 (1990)
22. W.A. Bardeen, Weak matrix elements in the large N_c limit, in *Proceedings KAON99*, pp. 171–176 (1999)
23. W.A. Bardeen, On the large N_c expansion in quantum chromodynamics. Fortsch. Phys. **50**, 483–488 (2002). [hep-ph/0112229]
24. M.A. Shifman, A. Vainshtein, V.I. Zakharov, Light quarks and the origin of the $\Delta I = 1/2$ rule in the nonleptonic decays of strange particles. Nucl. Phys. B **120**, 316 (1977)

25. S. Fajfer, J.-M. Gérard, A simple chiral Lagrangian approach to $K \to \pi\pi\pi$ decays and $\epsilon' + 0-$. Z. Phys. C **42**, 425 (1989)
26. J. Bijnens, J.-M. Gérard, G. Klein, The $K_L - K_S$ mass difference. Phys. Lett. B **257**, 191–195 (1991)
27. J. Bijnens, B. Guberina, Chiral perturbation theory and the evaluation of $1/N_c$ corrections to non-leptonic decays. Phys. Lett. B **205**, 103 (1988)
28. A. Pich, E. de Rafael, Weak K amplitudes in the chiral and 1/n(c) expansions. Phys. Lett. B **374**, 186–192 (1996). [hep-ph/9511465]
29. J. Bijnens, J. Prades, The B(K) parameter in the $1/N(c)$ expansion. Nucl. Phys. B **444**, 523–562 (1995). [hep-ph/9502363]
30. J. Bijnens, J. Prades, The $\Delta I = 1/2$ rule in the chiral limit. JHEP **9901**, 023 (1999). [hep-ph/9811472]
31. T. Hambye, G. Kohler, E. Paschos, P. Soldan, W.A. Bardeen, $1/N$ corrections to the hadronic matrix elements of Q_6 and Q_8 in $K \to \pi\pi$ decays. Phys. Rev. D **58**, 014017 (1998). [hep-ph/9802300]
32. T. Hambye, G. Kohler, P. Soldan, New analysis of the $\Delta I = 1/2$ rule in kaon decays and the $\hat{B}_K$ parameter. Eur. Phys. J. **C10**, 271–292 (1999). [hep-ph/9902334]
33. S. Peris, E. de Rafael, $K^0 - \bar{K}^0$ mixing in the $1/N(c)$ expansion. Phys. Lett. B **490**, 213–222 (2000). [hep-ph/0006146]
34. V. Cirigliano, J.F. Donoghue, E. Golowich, K. Maltman, Improved determination of the electroweak penguin contribution to ε'/ε in the chiral limit. Phys. Lett. B **555**, 71–82 (2003). [hep-ph/0211420]
35. T. Hambye, S. Peris, E. de Rafael, $\Delta I = 1/2$ and ϵ'/ϵ in large N(c) QCD. JHEP **0305**, 027 (2003). [hep-ph/0305104]
36. B. Lucini, M. Panero, SU(N) gauge theories at large N. Phys. Rep. **526**, 93–163 (2013). arXiv:1210.4997
37. RBC Collaboration, UKQCD Collaboration Collaboration, P. Boyle et al., Emerging understanding of the $\Delta I = 1/2$ rule from lattice QCD. Phys. Rev. Lett. **110**, 152001 (2013). arXiv:1210.4997
38. T. Blum, P. Boyle, N. Christ, N. Garron, E. Goode et al., $K \to \pi\pi$ Decay amplitudes from lattice QCD. Phys. Rev. D **84**, 114503 (2011). arXiv:1106.2714
39. T. Blum, P. Boyle, N. Christ, N. Garron, E. Goode et al., The $K \to (\pi\pi)_{I=2}$ decay amplitude from lattice QCD. Phys. Rev. Lett. **108**, 141601 (2012). arXiv:1111.1699
40. T. Blum, P. Boyle, N. Christ, N. Garron, E. Goode et al., Lattice determination of the $K \to (\pi\pi)_{I=2}$ decay amplitude A_2. Phys. Rev. D **86**, 074513 (2012). arXiv:1206.5142
41. C. Tarantino, Flavor lattice QCD in the precision era. PoS ICHEP2012, 023 (2013). arXiv:1210.0474
42. RBC-UKQCD Collaboration, C. T. Sachrajda, Prospects for lattice calculations of rare kaon decay amplitudes. PoS KAON13, 019 (2013)
43. N. Christ, Nonleptonic kaon decays from lattice QCD. PoS KAON13, 029 (2013)
44. N. Carrasco, V. Lubicz, L. Silvestrini, Vacuum insertion approximation and the $\Delta I = 1/2$ rule: a lattice QCD test of the naïve factorization hypothesis for K, D, B and static mesons. arXiv:1312.6691
45. M. Gavela, L. Maiani, S. Petrarca, F. Rapuano, G. Martinelli et al., The kaon B parameter and $K \to \pi$ and $K \to \pi\pi$ transition amplitudes on the lattice. Nucl. Phys. B **306**, 677 (1988)
46. J.-M. Gérard, An upper bound on the Kaon B-parameter and $\mathrm{Re}(\epsilon_K)$. JHEP **1102**, 075 (2011). arXiv:1012.2026
47. A. Soni, Lattice understanding of the $\Delta I = 1/2$ rule and some implications. arXiv:1311.6479
48. J.-M. Gérard, Vector meson effects on hadronic matrix elements. Talk given at ICHEP 1988
49. M. Fukugita, T. Inami, N. Sakai, S. Yazaki, Nonleptonic decays of kaons in the 1/N-C expansion. Phys. Lett. B **72**, 237 (1977)
50. H.P. Nilles, V. Visnjic-Triantafillou, Nonleptonic weak decays in QCD in two-dimensions. Phys. Rev. D **19**, 969 (1979)
51. D. Tadic, J. Trampetic, Weak meson decays and the 1/N expansion. Phys. Lett. B **114**, 179 (1982)
52. A.J. Buras, J.-M. Gérard, R. Rückl, 1/N expansion for exclusive and inclusive charm decays. Nucl. Phys. B **268**, 16 (1986)
53. M. Wirbel, B. Stech, M. Bauer, Exclusive semileptonic decays of heavy mesons. Z. Phys. C **29**, 637 (1985)
54. B.D. Gaiser, T. Tsao, M.B. Wise, Parameters of the six quark model. Ann. Phys. **132**, 66 (1981)
55. L. Giusti, P. Hernandez, M. Laine, P. Weisz, H. Wittig, A strategy to study the role of the charm quark in explaining the $\Delta I = 1/2$ rule. JHEP **0411**, 016 (2004). [hep-lat/0407007]
56. E. Endress, C. Pena, Contribution of the charm quark to the $\Delta I = 1/2 rule$. PoS Confinement X, 110 (2012). arXiv:1212.4642
57. N. Christ, T. Izubuchi, C. Sachrajda, A. Soni, J. Yu, Long distance contribution to the $K_L - K_S$ mass difference. arXiv:1212.5931
58. A.J. Buras, M. Jamin, M.E. Lautenbacher, The anatomy of ε'/ε beyond leading logarithms with improved hadronic matrix elements. Nucl. Phys. B **408**, 209–285 (1993). [hep-ph/9303284]
59. M. Ciuchini, E. Franco, G. Martinelli, L. Reina, The $\Delta S = 1$ effective Hamiltonian including next-to-leading order QCD and QED corrections. Nucl. Phys. B **415**, 403–462 (1994). [hep-ph/9304257]
60. A.J. Buras, P. Gambino, U.A. Haisch, Electroweak penguin contributions to nonleptonic $\Delta F = 1$ decays at NNLO. Nucl. Phys. B **570**, 117–154 (2000). [hep-ph/9911250]
61. M. Gorbahn, U. Haisch, Effective Hamiltonian for non-leptonic $|DeltaF| = 1$ decays at NNLO in QCD. Nucl. Phys. B **713**, 291–332 (2005). [hep-ph/0411071]
62. G. Buchalla, A.J. Buras, M.E. Lautenbacher, Weak decays beyond leading logarithms. Rev. Mod. Phys. **68**, 1125–1144 (1996). [hep-ph/9512380]
63. S.R. Coleman, E. Witten, Chiral symmetry breakdown in large N chromodynamics. Phys. Rev. Lett. **45**, 100 (1980)
64. E. Witten, Anti-de Sitter space, thermal phase transition, and confinement in gauge theories. Adv. Theor. Math. Phys. **2**, 505–532 (1998). [hep-th/9803131]
65. J. Polchinski, M.J. Strassler, Hard scattering and gauge/string duality. Phys. Rev. Lett. **88**, 031601 (2002). [hep-th/0109174]
66. T. Hambye, B. Hassanain, J. March-Russell, M. Schvellinger, On the $\Delta I = 1/2$ rule in holographic QCD. Phys. Rev. D **74**, 026003 (2006). [hep-ph/0512089]
67. T. Hambye, B. Hassanain, J. March-Russell, M. Schvellinger, Four-point functions and kaon decays in a minimal AdS/QCD model. Phys. Rev. D **76**, 125017 (2007). [hep-ph/0612010]
68. R.S. Chivukula, J. Flynn, H. Georgi, Polychromatic penguins don't fly. Phys. Lett. B **171**, 453–458 (1986)
69. J. Gasser, H. Leutwyler, Chiral perturbation theory to one loop. Ann. Phys. **158**, 142 (1984)
70. M. Bando, T. Kugo, K. Yamawaki, Nonlinear realization and hidden local symmetries. Phys. Rep. **164**, 217–314 (1988)
71. G. Ecker, J. Gasser, H. Leutwyler, A. Pich, E. de Rafael, Chiral Lagrangians for massive spin 1 fields. Phys. Lett. B **223**, 425 (1989)
72. W.A. Bardeen, J. Bijnens, J.-M. Gérard, Hadronic matrix elements and the $\pi^+\pi^0$ mass difference. Phys. Rev. Lett. **62**, 1343 (1989)
73. J. Fatelo, J.-M. Gérard, Current-current operator evolution in the chiral limit. Phys. Lett. B **347**, 136–142 (1995)
74. A.J. Buras, Weak Hamiltonian, CP violation and rare decays, in *Probing the Standard Model of Particle Interactions*, ed. by F. David, R. Gupta (Elsevier Science B.V., 1998). hep-ph/9806471
75. A.J. Buras, M. Jamin, P.H. Weisz, Leading and next-to-leading QCD corrections to ϵ parameter and $B^0 - \bar{B}^0$ mixing in the presence of a heavy top quark. Nucl. Phys. B **347**, 491–536 (1990)
76. J.F. Donoghue, E. Golowich, B.R. Holstein, The $\Delta S = 2$ matrix element for $K^0 - \bar{K}^0$ mixing. Phys. Lett. B **119**, 412 (1982)

77. A. Pich, E. De Rafael, K anti-K mixing in the standard model. Phys. Lett. B **158**, 477–484 (1985)
78. Y. Aoki, R. Arthur, T. Blum, P. Boyle, D. Brommel et al., Continuum limit of B_K from 2+1 flavor domain wall QCD. Phys. Rev. D **84**, 014503 (2011). arXiv:1012.4178
79. T. Bae, Y.-C. Jang, C. Jung, H.-J. Kim, J. Kim et al., B_K using HYP-smeared staggered fermions in $N_f = 2 + 1$ unquenched QCD. Phys. Rev. D **82**, 114509 (2010). arXiv:1008.5179
80. ETM Collaboration Collaboration, M. Constantinou et al., B_K-parameter from $N_f = 2$ twisted mass lattice QCD. Phys. Rev. D **83**, 014505 (2011). arXiv:1009.5606]
81. G. Colangelo, S. Durr, A. Juttner, L. Lellouch, H. Leutwyler et al., Review of lattice results concerning low energy particle physics. Eur. Phys. J. C **71**, 1695 (2011). arXiv:1011.4408
82. J.A. Bailey, T. Bae, Y.-C. Jang, H. Jeong, C. Jung, et al., Beyond the standard model corrections to $K^0 - \bar{K}^0$ mixing. PoS LATTICE2012, 107 (2012). arXiv:1211.1101
83. S. Durr, Z. Fodor, C. Hoelbling, S. Katz, S. Krieg, et al., Precision computation of the kaon bag parameter. Phys. Lett. B **705**, 477–481 (2011). arXiv:1106.3230
84. T. Bae, Y.-C. Jang, H. Jeong, J. Kim, J. Kim, et al., Update on B_K and ε_K with staggered quarks. (2011)
85. J. Frison, P. Boyle, N. H. Christ, N. Garron, R. Mawhinney, et al., The kaon bag parameter at physical mass. arXiv:1312.2374
86. SWME Collaboration Collaboration, T. Bae et al., Improved determination of B_K with staggered quarks. arXiv:1402.0048
87. A.J. Buras, J.-M. Gérard, ε'/ε in the Standard Model. Phys. Lett. B **203**, 272 (1988)
88. S. Aoki, Y. Aoki, C. Bernard, T. Blum, G. Colangelo, et al., Review of lattice results concerning low energy particle physics. arXiv:1310.8555
89. A.J. Buras, J.-M. Gérard, Isospin breaking contributions to ε'/ε. Phys. Lett. B **192**, 156 (1987)
90. V. Cirigliano, A. Pich, G. Ecker, H. Neufeld, Isospin violation in ϵ'. Phys. Rev. Lett. **91**, 162001 (2003). [hep-ph/0307030]
91. M. Gaillard, B.W. Lee, $\Delta I = 1/2$ rule for nonleptonic decays in asymptotically free field theories. Phys. Rev. Lett. **33**, 108 (1974)
92. G. Altarelli, L. Maiani, Octet enhancement of nonleptonic weak interactions in asymptotically free gauge theories. Phys. Lett. B **52**, 351–354 (1974)
93. J.-M. Gérard, J. Weyers, Trace anomalies and the $\Delta I = 1/2$ rule. Phys. Lett. B **503**, 99–103 (2001). [hep-ph/0011391]
94. R. Crewther, L.C. Tunstall, $\Delta I = 1/2$ Rule for kaon decays derived from QCD infrared fixed point. arXiv:1312.3319
95. J. Brod, M. Gorbahn, Next-to-next-to-leading-order charm-quark contribution to the CP violation parameter ε_K and ΔM_K. Phys. Rev. Lett. **108**, 121801 (2012). arXiv:1108.2036
96. A.J. Buras, J. Girrbach, Stringent tests of constrained minimal flavour violation through $\Delta F = 2$ transitions. Eur. Phys. J. C **9**(73) (2013). arXiv:1304.6835
97. S. Herrlich, U. Nierste, Enhancement of the $K_L - K_S$ mass difference by short distance QCD corrections beyond leading logarithms. Nucl. Phys. B **419**, 292–322 (1994). [hep-ph/9310311]
98. M. Gaillard, B.W. Lee, Rare decay modes of the K-mesons in gauge theories. Phys. Rev. D **10**, 897 (1974)
99. J.-M. Gérard, C. Smith, S. Trine, Radiative kaon decays and the penguin contribution to the $\Delta I = 1/2$ rule. Nucl. Phys. B **730**, 1–36 (2005). [hep-ph/0508189]
100. J.-M. Gérard, P. Mertens, Weakly-induced strong CP-violation. Phys. Lett. B **716**, 316–321 (2012). arXiv:1206.0914
101. A.J. Buras, D. Guadagnoli, G. Isidori, On ϵ_K beyond lowest order in the Operator product expansion. Phys. Lett. B **688**, 309–313 (2010). arXiv:1002.3612